Available online at www.sciencedirect.com
SCIENCE DIRECT®
ELSEVIER
Palaeogeography, Palaeoclimatology, Palaeoecology 234 (2006) 304–327
PALAEO
www.elsevier.com/locate/palaeo

Hydrographic development of the Aral Sea during the last 2000 years based on a quantitative analysis of dinoflagellate cysts

P. Sorrel [a,b,*], S.-M. Popescu [b], M.J. Head [c,1], J.P. Suc [b], S. Klotz [b,d], H. Oberhänsli [a]

[a] *GeoForschungsZentrum, Telegraphenberg, D-14473 Potsdam, Germany*
[b] *Laboratoire PaléoEnvironnements et PaléobioSphère (UMR CNRS 5125), Université Claude Bernard—Lyon 1, 27-43, boulevard du 11 Novembre, 69622 Villeurbanne Cedex, France*
[c] *Department of Geography, University of Cambridge, Downing Place, Cambridge CB2 3EN, UK*
[d] *Institut für Geowissenschaften, Universität Tübingen, Sigwartstrasse 10, 72070 Tübingen, Germany*

Received 30 June 2005; received in revised form 4 October 2005; accepted 13 October 2005

Abstract

The Aral Sea Basin is a critical area for studying the influence of climate and anthropogenic impact on the development of hydrographic conditions in an endorheic basin. We present organic-walled dinoflagellate cyst analyses with a sampling resolution of 15 to 20 years from a core retrieved at Chernyshov Bay in the NW Large Aral Sea (Kazakhstan). Cysts are present throughout, but species richness is low (seven taxa). The dominant morphotypes are *Lingulodinium machaerophorum* with varied process length and *Impagidinium caspienense*, a species recently described from the Caspian Sea. Subordinate species are *Caspidinium rugosum*, *Romanodinium areolatum*, *Spiniferites cruciformis*, cysts of *Pentapharsodinium dalei*, and round brownish protoperidiniacean cysts. The chlorococcalean algae *Botryococcus* and *Pediastrum* are taken to represent freshwater inflow into the Aral Sea.

The data are used to reconstruct salinity as expressed in lake level changes during the past 2000 years. We quantify and date for the first time prominent salinity variations from the northern part of the Large Aral Sea. During high lake levels, *I. caspienense*, representing brackish conditions with salinities of about 10–15 g kg^{-1} or less, prevails. Assemblages dominated by *L. machaerophorum* document lake lowstands during approximately 0–425 AD (or 100? BC–425 AD), 920–1230 AD, 1500 AD, 1600–1650 AD, 1800 AD and since the 1960s. Because salinity in the Aral Sea is mostly controlled by meltwater discharges from the Syr Darya and Amu Darya rivers, we interpret changes in salinity levels as a proxy for temperature fluctuations in the Tien Shan Mountains that control snow melt. Significant erosion of marine Palaeogene and Neogene deposits in the hinterland, evidenced between 1230 AD and 1400 AD, is regarded as sheet-wash from shore. This is controlled by the low pressure system that develops over the Eastern Mediterranean and brings moist air to the Middle East and Central Asia during late spring and summer. We propose that the recorded environmental changes are related primarily to climate, but perhaps to a lesser extent by human-controlled irrigation activities. Our results documenting climate change in western Central Asia are fairly consistent with reports elsewhere from Central Asia.

Keywords: Aral Sea hydrology; Late Holocene; Dinoflagellate cysts; Lake level changes; Glacial meltwater discharge; Mediterranean low-pressure system

* Corresponding author. GeoForschungsZentrum, Telegraphenberg, D-14473 Potsdam, Germany. Tel.: +49 331 288 1347; fax: +49 331 288 1349.
E-mail address: psorrel@gfz-potsdam.de (P. Sorrel).
[1] Present address: Department of Earth Sciences, Brock University, 500 Glenridge Avenue, St. Catharines, Ontario, Canada L2S 3A1.

0031-0182/$ - see front matter © 2006 Elsevier B.V. All rights reserved.
doi:10.1016/j.palaeo.2005.10.012

1. Introduction

The Aral Sea is a large saline lake in the Aral–Sarykamish depression in Central Asia and bordered by Kazakhstan and Uzbekistan (Fig. 1). After about 14 ka, when the Aral and Caspian seas became separated from one another (Tchepaliga, 2004), the Aral Sea level developed a strong dependence upon the inflow of its two main tributaries, the Syr Darya and Amu Darya rivers. These rivers originate from the

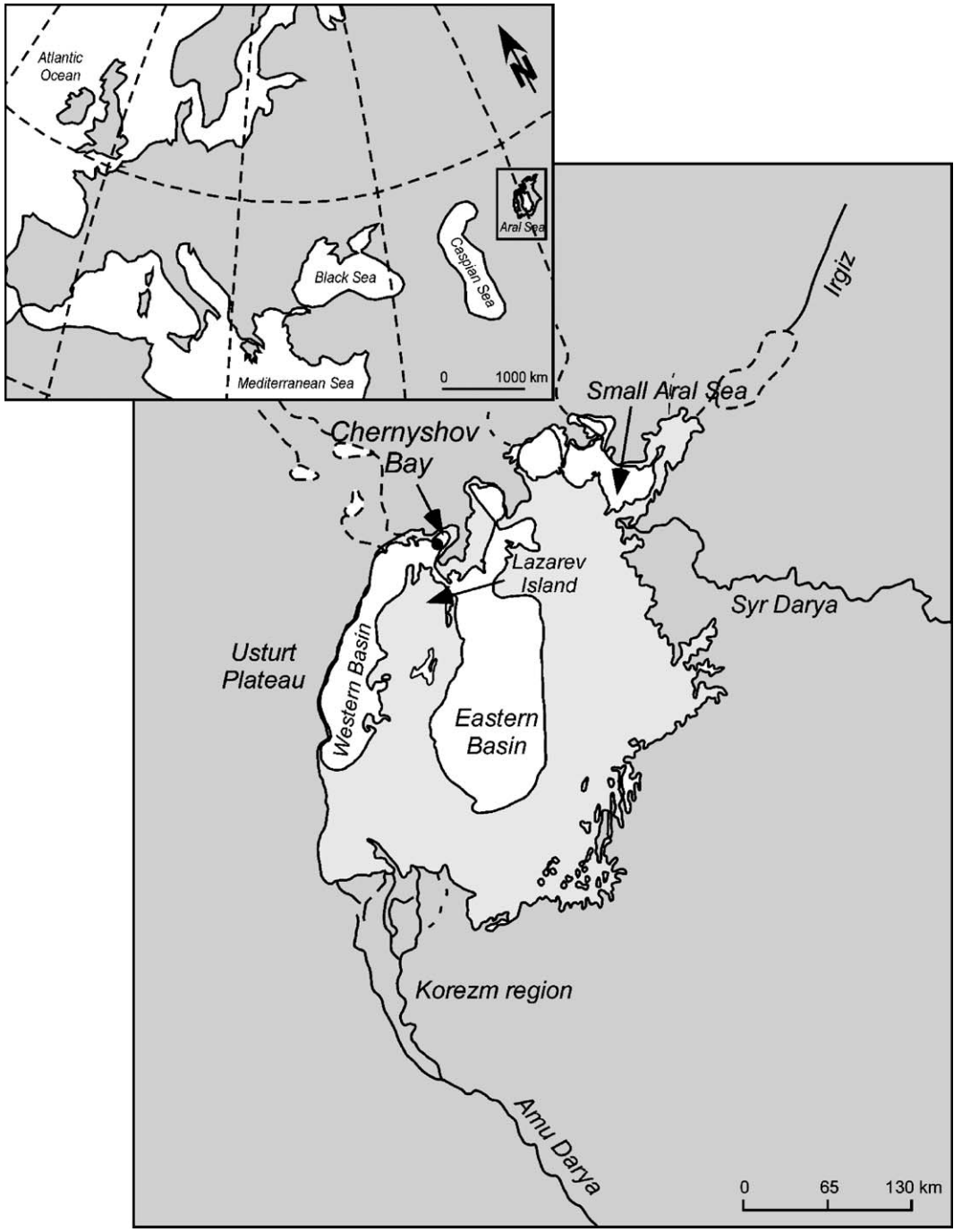

Fig. 1. Location map of the present Aral Sea (in white) and the study area. The light grey shading indicates the sea level from the early 1960s, whereas the dashed lines represent the former courses of episodic local rivers (after Létolle and Mainguet, 1993). The Eastern and Western basins constitute the Large Aral Sea.

highest part of the Pamir and Tien Shan mountains, 1500 km southeast of the Aral Sea. Nowadays, the Aral Sea is an endorheic lake with low freshwater inflow from rivers and low precipitation due to the extremely arid continental climate (~100 mm year^{-1} on average; Létolle and Mainguet, 1993). As a result of extreme insolation-forced heating leading to desert conditions, the mechanical and chemical weathering of sediments is accentuated and erosional processes are enhanced.

During the past 40 years the Aral Sea, which was the fourth largest inland lake in the world, has suffered a dramatic reduction in size due to intensive irrigation activities in the hinterland (Boomer et al., 2000). As a consequence, its area has diminished more than fourfold, and the volume more than tenfold. The lake level has in fact stabilised during the last 3 to 4 years, as irrigation has decreased (Zavialov, 2005). Nonetheless, the lake level dropped by 22.5 m from its value in 1965, and the Aral Sea became split into two major water bodies, namely the Large Aral Sea represented by its western and eastern basins which are connected only through a short (3 km) and shallow (8 m) channel (Nourgaliev, pers. comm. in Zavialov, 2005), and the Small Aral Sea in the North (Fig. 1). Today, the lake level is at 30.5 m above sea level (a.s.l.) (Zavialov et al., 2003), whereas it was at 53 m a.s.l. in 1960 (Létolle and Mainguet, 1993). As a result of the considerable reduction in water volume and the reduced freshwater influx into the Aral Sea, salinity levels have increased more than eightfold. Surface-water salinity rose from 10.4 g kg^{-1} in 1960 to more than 80 g kg^{-1} in 2002–2003 (Zavialov et al., 2003; Friedrich and Oberhänsli, 2004). The salinification had recently considerable consequences for the flora and fauna (Mirabdullayev et al., 2004), thus showing that the Aral Sea represents an ecosystem highly sensitive to climate changes and anthropogenic impact.

The palaeoenvironmental development of the Aral Sea has been studied from sediments since the late 1960s. Maev et al. (1999) dated changes in palaeoenvironmental conditions over the past 7000 years from two cores retrieved in the central part of the eastern basin. They reported phases of major regression during approximately 450–550 AD and 1550–1650 AD. This was further confirmed by Aleshinskaya et al. (1996) using palaeontological proxies and by Boroffka et al. (2005) from archaeological and geomorphological observations. Boroffka et al. (2005) also documented a low lake level from 800 AD to 1100 AD. However, interpretation remains ambiguous for the time window 1000–1500 AD. Aleshinskaya et al. (1996) suggested deep-water conditions between 1100 AD and 1500 AD, whereas historical data point to a severe (or even complete) drying-out of the lake between the 13th and the 16th centuries (Boroffka et al., 2005).

Regarding environmental changes during the Holocene, the present state of knowledge is fairly good for the region south of the Aral Sea but rather poor for the northern part. During a field campaign in the summer of 2002, sediment cores were retrieved for the first time from the northwest shore of the Large Aral Sea (Chernyshov Bay; Fig. 1) (www.CLIMAN.gfz-potsdam.de). Using this cored material, we present new palaeontological data covering the past 2000 years with a time resolution of 15 to 20 years. Based on a quantitative analysis of organic-walled dinoflagellate cysts, we provide evidence for large palaeosalinity and lake water level variations.

2. Material and methods

2.1. Sedimentological description

In August 2002, two piston cores (composite cores CH1 and CH2 with respective total lengths of 11.04 m and 6.0 m) taken with a Usinger piston corer (http://CLIMAN.gfz-potsdam.de) and six gravity cores were retrieved from Chernyshov Bay (Fig. 1). These cores were collected 1 km from the shoreline (45°58′528″N, 59°14′459″E) at a water depth of 22 m. Composite Core CH1 consists of sections 21, 22, 23, 27, 28 and 29, whereas composite core CH2 consists of sections 30, 31 and 32. Cores CH1 and CH2 were retrieved from the same coring location at about 1m apart. In this study, we conducted our analyses on sections 30, 31 and 32 from Core CH2 and on sections 27, 28 and 29 from Core CH1. We then named this composite section CH2/1, whose total length is 10.79 m. The correlation between Cores CH1 and CH2 was performed by matching laminations using photographs, physical properties (bulk sediment density, magnetic susceptibility) and XRF scanning.

Sediments from this site (Fig. 2A) consist of greenish to greyish silty clays and dark water-saturated organic muds with sporadically intercalated more sandy material. The sediments, which are finely laminated, comprise material of variable origin (terrigenous, biogenic and chemogenic) and size (from clay and fine silt to fine sand with mollusc shell fragments). Chemical precipitates, such as gypsum (G), occur both as dispersed microcrystals in the sediment (G_3, G_4; Fig. 2B) and as discrete layers (G_1, G_2). Neither erosive discontinuity, nor features of bottom traction are ob-

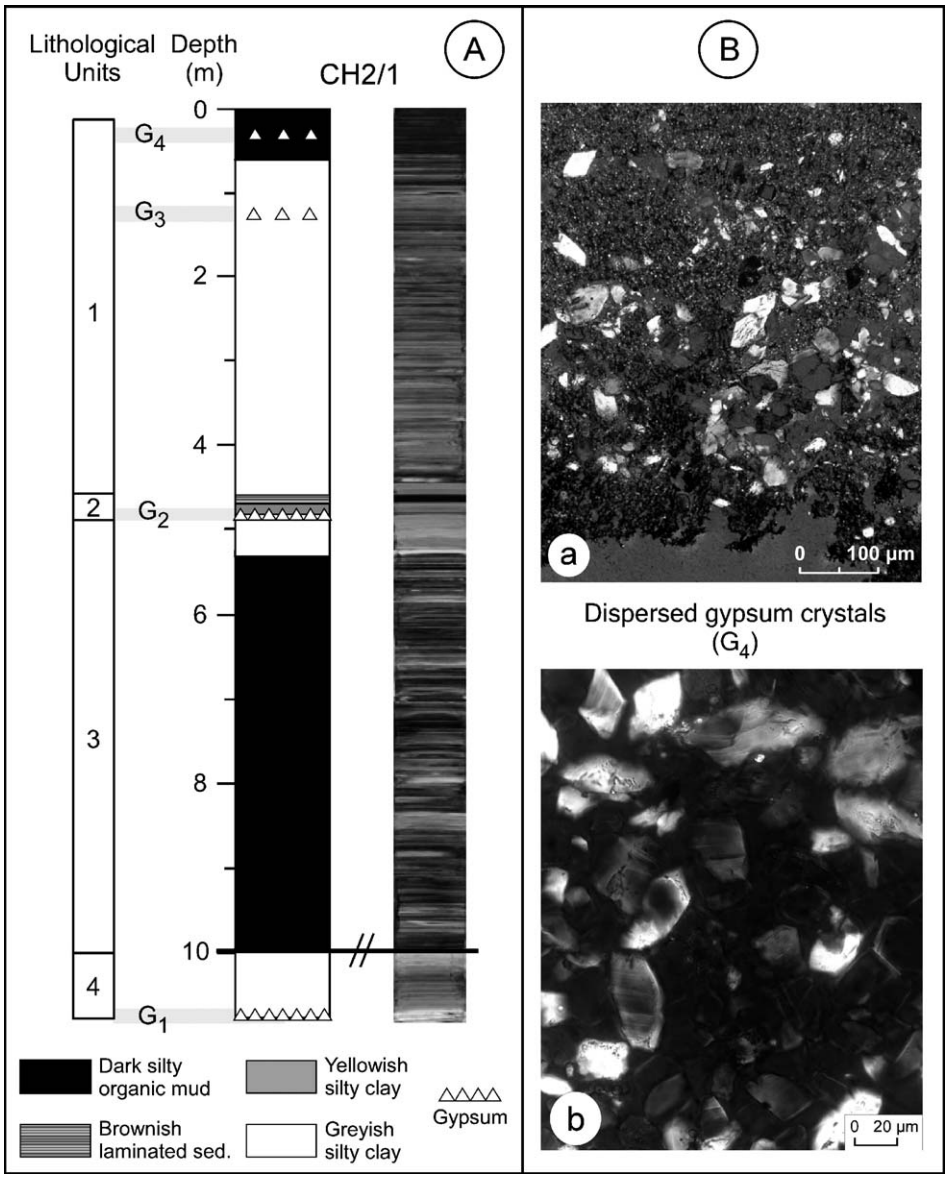

Fig. 2. A: Lithology of section CH2/1 (total depth = 10.79 m). Note the break in core between Units 3 and 4 corresponding to a coring gap of unknown extent. B: Microfacies photographs. a: Dispersed gypsum crystals in a fine clayey matrix (G_4 [0.2–0.3 m]); b: Gypsum crystals showing characteristic monoclinic structures and cleavages (G_4 [0.2–0.3 m]).

served in the core. The laminated character of section CH2/1 indicates probable settling of various autochthonous and allochthonous particles from the water column during seasonally varying hydrographic conditions. Four lithological units are recognized. Between 0.0 and 4.5 m (Unit 1), the sediment is mostly silty to sandy clay with rare macrofossil remains although the uppermost part (0.0–0.5 m) consists of a dark, organic, finely laminated mud. Unit 2 is characterized by a horizon of laminated gypsum at its base (G_2: 1-cm thick) overlain by a 13-cm thick interval of yellowish thinly laminated sediments which in turn are abruptly interrupted by brownish laminated sediments (10.5-cm thick interval). Downcore, between 4.86 and 9.7 m depth (Unit 3), the sediments consist of a dark silty organic mud, often water-saturated and very rich in organic matter including allochthonous aquatic plant remains. The plant remains occur both as a dispersed phase in the matrix and as partly decayed fragments that constitute organic horizons. These sediments, which are characteristic of dysoxic to anoxic bottom-water conditions, are separated from a lower sequence

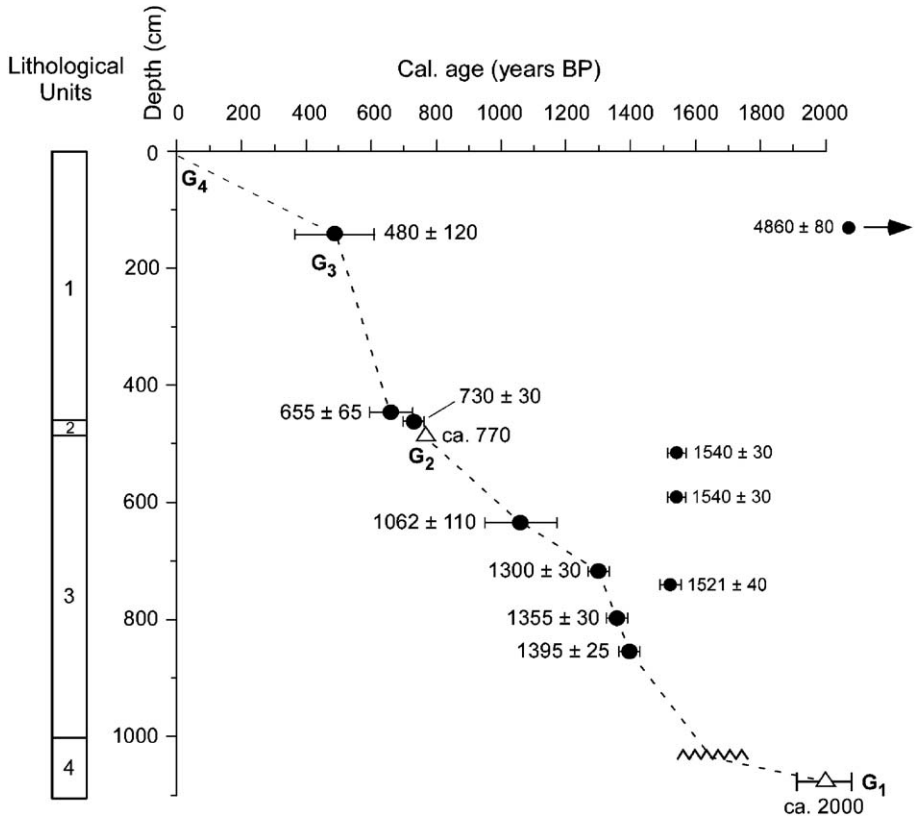

Fig. 3. Age model for section CH2/1 based on AMS ^{14}C dating on the filamentous green alga *Vaucheria* sp.: 480 ± 120 cal. yr BP, 655 ± 65 cal. yr BP (Nourgaliev et al., 2003); 108.6 ± 0.3 pMC (Poz-4753), 1062 ± 110 yr BP (Poz-12279), 1300 ± 30 cal. yr BP (Poz-4762), 1395 ± 25 cal. yr BP (Poz-4760), 1521 ± 40 cal. yr BP (Poz-4764), 1540 ± 30 cal. yr BP (Poz-4756/59), 4860 ± 80 cal. yr BP (Poz-4760), on TOC: 730 ± 30 yr BP (Poz-13511), and on $CaCO_3$ of mollusc shells: 1355 ± 30 cal. yr BP (Poz-9662). AMS ^{14}C dating was measured in the Poznań Radiocarbon Laboratory (Poland).

(9.97–10.79 m, Unit 4) by a coring gap of unknown extent. Unit 4 consists of thinly laminated grey silty clays that include at the base, laminated gypsum (G_1) interbedded with clayey layers. No turbiditic sediments have been recognized. The hydrochemical conditions at Chernyshov Bay today are very pronounced. A strong pycnocline has developed that maintains and stabilises an underlying body of anoxic deep-water (Friedrich and Oberhänsli, 2004) that in turn influences sedimentation by preventing bioturbation (except in the topmost part of the core [0.0–0.05 m]). Hence, sediments from Chernyshov Bay show well-preserved laminations (Friedrich and Oberhänsli, 2004).

2.2. Age model

In section CH2/1, AMS radiocarbon ages were determined using the filamentous green alga *Vaucheria* sp. and $CaCO_3$ from mollusc shells which were picked from the sediment sample and carefully washed. Algae were stored in water within a glass vessel. For each sample, AMS ^{14}C dating was performed using between 0.2 and 1.0 mg of pure extracted carbon. Radiocarbon ages were corrected to calibrated (cal) ages using the IntCal04 calibration curve published in Reimer et al. (2004). These determinations resulted in sedimentation rate estimates for

Fig. 4. Relative abundance of dinoflagellate cysts and freshwater algae from the Chernyshov Bay Core CH2/1, ecostratigraphic zonation based on the dinoflagellate cysts, and schematic salinity fluctuations. Each species and morphotype is expressed as a proportion of the total in-situ dinoflagellate cysts. *Pediastrum* sp. and *Botryococcus braunii*-type are expressed as a proportion of the total in-situ dinoflagellate cysts plus freshwater taxa. Reworked dinoflagellate cysts are expressed as a proportion of total in-situ dinoflagellate cysts plus reworked dinoflagellate cysts. Solid dots indicate rare occurrence (0.5% or less). Each sample represents a ~10 cm interval of core and is plotted by its mean depth. Oligosaline conditions represent salinities of 0.5–5 g kg^{-1}; mesosaline conditions salinities of 5–20 g kg^{-1} and poly- to meta-/hypersaline conditions salinities >20/30 g kg^{-1}. See Fig. 2 for explanation of lithology.

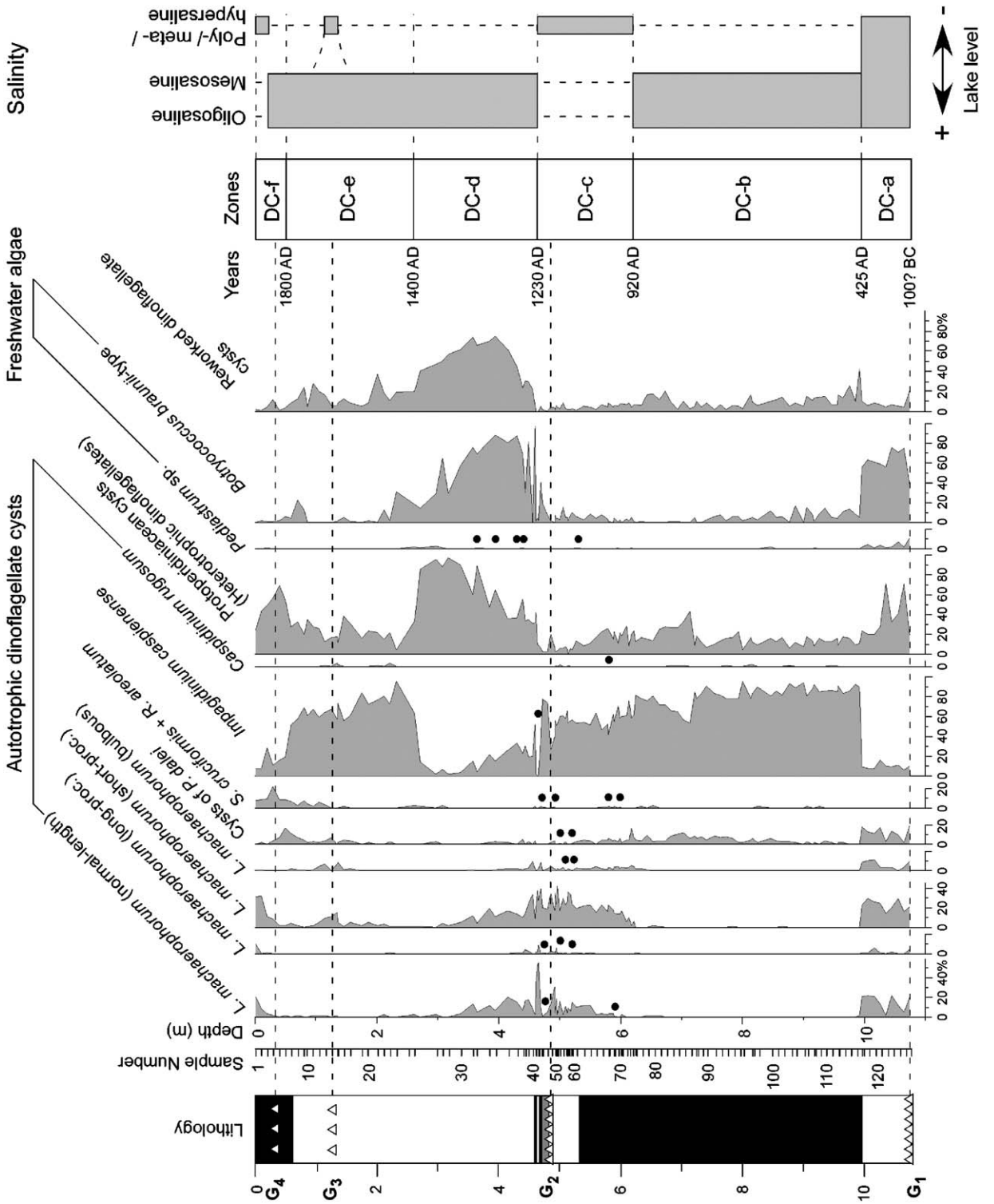
Salinity
Poly-/ meta- / hypersaline
Mesosaline
Oligosaline
Lake level
Zones
DC-f
DC-e
DC-d
DC-c
DC-b
DC-a
Years
1800 AD
1400 AD
1230 AD
920 AD
425 AD
100? BC
Freshwater algae
Reworked dinoflagellate cysts
Botryococcus braunii-type
Pediastrum sp.
Autotrophic dinoflagellate cysts
(Heterotrophic dinoflagellates)
Protoperidiniacean cysts
Caspidinium rugosum
Caspidinium caspiense
Impagidinium + R. areolatum
S. cruciformis
Cysts of P. dalei
L. machaerophorum (bulbous)
L. machaerophorum (short-proc.)
L. machaerophorum (long-proc.)
L. machaerophorum (normal-length)
Depth (m)
Sample Number
Lithology
G4
G3
G2
G1

the different lithological units. A preliminary age model for section CH2/1 based on AMS radiocarbon dating is proposed in Fig. 3. Reliable dating for the upper 6 m of section CH2/1 was obtained by correlation with the magnetic susceptibility record from parallel cores 7, 8 and 9 retrieved 50 m apart from the studied cores (Nourgaliev et al., 2003). AMS ^{14}C dating on cores 7, 8 and 9 was performed on the green alga *Vaucheria* sp. This correlation gives an age of 480 ± 120 years BP (cal. years) at 1.4 m depth for section CH2/1. In addition, the time interval represented by Unit 2 is temporally constrained between 655 ± 65 years BP (cal. years) at 4.5 m depth and 770 yr BP at 4.86 m for the laminated gypsum, as correlated to a decrease in tree-ring width from the Tien Shan Mountains (see Fig. 11). This time range is further constrained by an age of 730 ± 30 yr BP (cal. years) at 4.65 m. These results imply high sedimentation rates during the deposition of Unit 1 (1.6 cm year^{-1} from 1.36 m to 4.43 m) but conversely very low sedimentation rates for Unit 2 (~0.3 cm year^{-1}). Supplementary ^{14}C dating performed on *Vaucheria* sp. provides an age of 1062 ± 110 cal. years BP at 6.34 m, 1300 ± 30 cal. years BP at 6.94 m and of 1395 ± 25 cal. years BP at 8.25 m, while ^{14}C dating from mollusc shells indicates an age of 1355 ± 30 years BP at 7.73 m. Relatively high sedimentation rates are implied for Unit 3 (~1.4 cm year^{-1} from 5.69 m to 10.36 m). Based on this adjustment, a linear extrapolation along Unit 3 would suggest an average age of ca. 2000 years BP (100? BC to 100 AD) for the base of section CH2/1 (G_4) corresponding to a major lake level drop. This is consistent with others studies (see Aleshinskaya et al., 1996 on radiocarbon-dated cores 15 and 86 from the Large Aral, and Boomer et al., 2000, p. 1269) that report on an important lake regression at 2000 years BP. Accordingly, a sampling interval of 10 cm, which represents a time resolution of 15 to 20 years, was selected. The top of the core (uppermost 40 cm) has been dated as post-1963, as based on a peak in ^{137}Cs at 0.44 m reflecting the climax of the bomb period (ca. 1963–1964 AD) (Heim, 2005) and this is confirmed by a date on *Vaucheria* sp. that reveals an age of 108.6 ± 0.3 pMC at 0.47 m. The dates 4860 ± 80 years BP at 1.30 m, 1540 ± 30 years BP at 5.16 m, 1540 ± 30 years BP at 5.90 m and 1521 ± 40 years BP at 7.40 m, respectively, reflect reworking of older material from shore. This is confirmed by reworked dinoflagellate cysts that are conspicuously abundant at these depths (see Fig. 4). Ages between 1521 and 1540 years BP typically represent sediment ages of a high lake-level stand. Due to a lack of dating of living algae sampled from the nearshore, no reservoir correction can be applied yet. This is work in progress.

2.3. Sample processing and palynological analysis

For the study of dinoflagellate cysts, 125 sediment samples each consisting of 15 to 25 g dry weight were treated sequentially with cold HCl (35%), cold HF (70%) and cold HCl (35%) after Cour's method (1974). Denser particles were then separated from the organic residue using $ZnCl_2$ (density = 2.0). After additional washing with HCl and water, the samples were sieved at 150 μm to eliminate the coarser particles including macro-organic remains, and then sieved again at 10 μm following brief (about 30 s) sonication. The residue was then stained using safranin-o, homogenized, and mounted onto microscope slides using glycerol. Finally, the coverslips were sealed with LMR histological glue.

Dinoflagellate cysts was identified and enumerated under a light microscope at × 1000 magnification. Between 200 and 400 dinoflagellate cysts were counted for intervals of elevated salinity since specimens are generally abundant in such intervals. In other slides, where dinoflagellate cysts occur very sparsely, a minimum of 100 dinoflagellate cysts per sample were counted. Light photomicrographs (LM) were taken using a Leica DMR microscope fitted with a Leica DC300 digital camera. For scanning electron micrographs, residues were sieved at 20 μm, washed with distilled water and air-dried onto small circular metal blocks for 2 h, mounted onto metal stubs, and sputter-coated with gold.

Calculation of dinoflagellate cyst concentrations per gram of dry sediment was performed according to Cour's method (1974). Dinoflagellate cysts were found in every sample examined and preservation varies from poor (crumpling of cysts) to very good in intervals of elevated salinity. The dinoflagellate cyst record is shown by relative abundances of each taxon in a detailed diagram to emphasize palaeoenvironmental changes in the core (Fig. 4). Also shown are concentrations of in-situ cysts (per gram dry weight) of other palynomorphs and of reworked taxa (Fig. 5). Counts are archived at the Laboratory 'PaléoEnvironnements et PaléobioSphère' (University Claude Bernard—Lyon 1, France). The dinoflagellate cyst zones (DC-a–DC-f; Figs. 4 and 5) have been established using Statistica 6.0 according to a canonical correspondence analysis performed on selected taxa representing variables, in order to determine major ecological trends across section CH2/1. In addition, to examine whether relative abundance could be

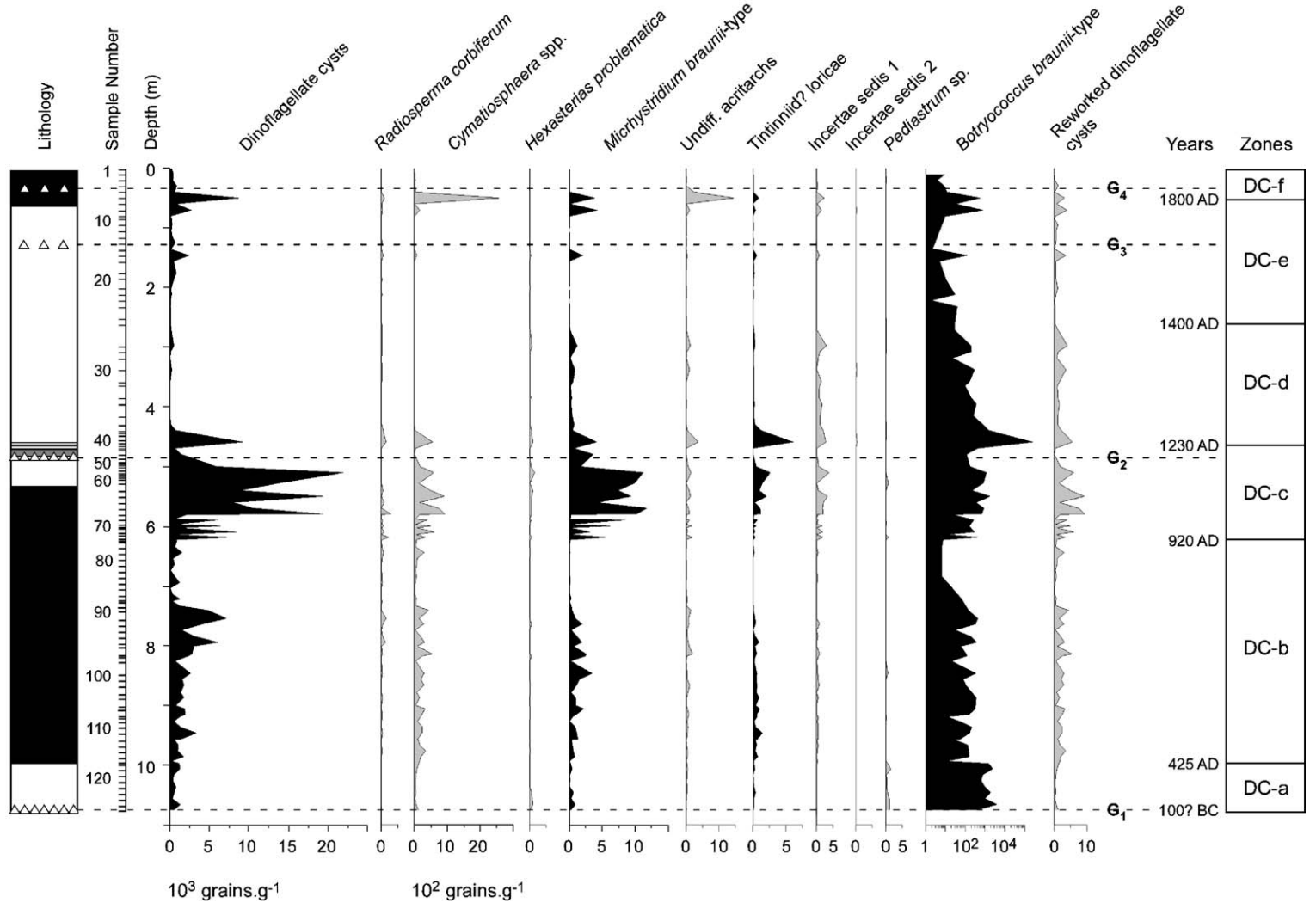

Fig. 5. Concentrations (per gram of dry sediment) of all aquatic palynomorphs counted in section CH2/1. Black-shaded curves: 10^3 grains g^{-1}. Grey-shaded curves: 10^2 grains g^{-1}. Note that concentrations of *Botryococcus braunii*-type are expressed in a logarithmic scale. Each sample represents a ~10 cm interval of core and is plotted by its mean depth. The zones refer to the dinoflagellate cyst ecostratigraphy described herein. See Fig. 2 for explanation of lithology.

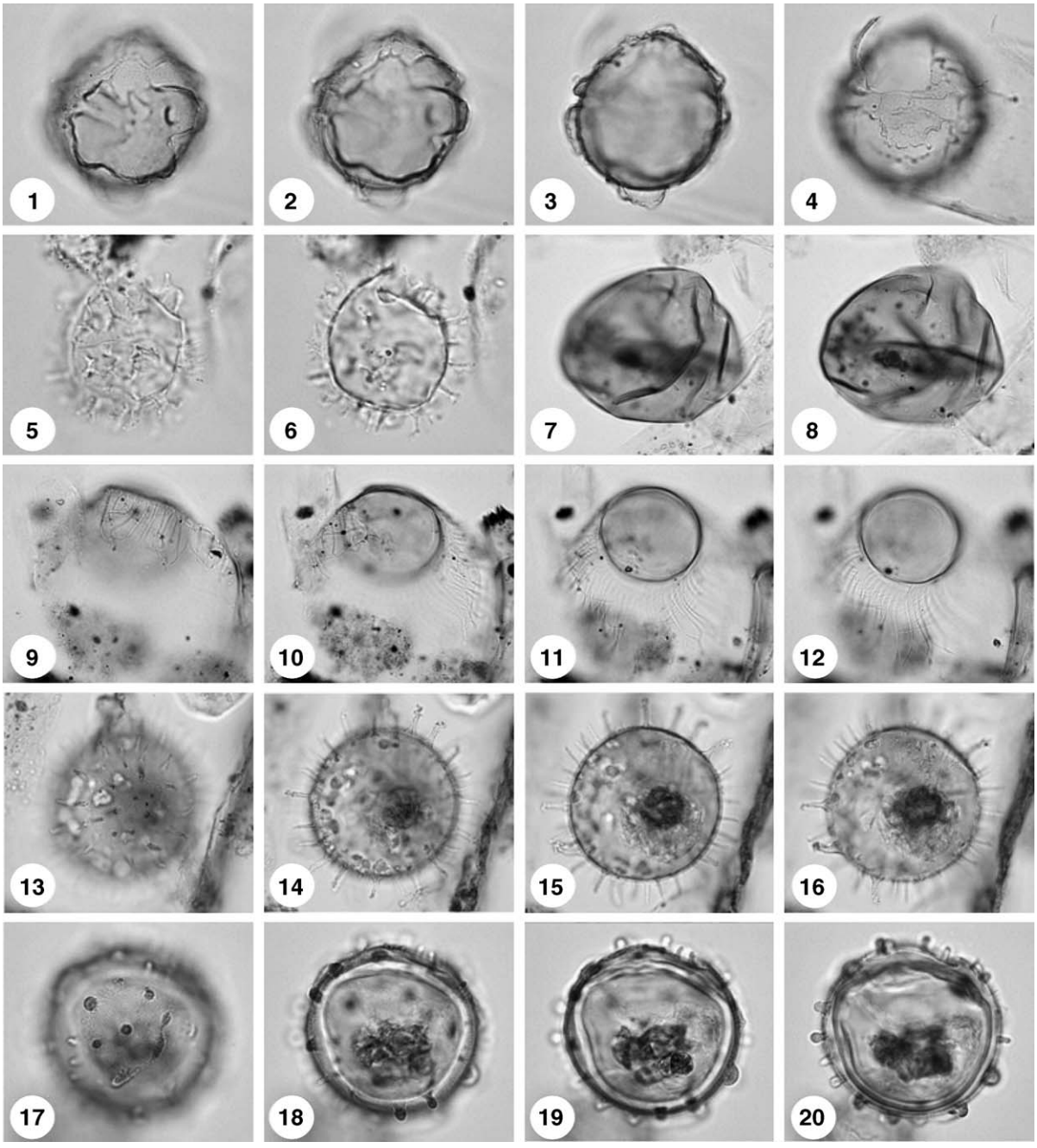

Fig. 6. Dinoflagellate cysts and other aquatic palynomorphs from Chernyshov Bay. Light micrographs in bright-field. An England Finder reference is given after the sample number. (1–4) *Impagidinium caspienense* Marret, 2004. Ventral view of ventral surface (1–2), mid-focus (3), and dorsal surface (4) showing archeopyle; max. dia. 45 μm; sample 1A (M20/3); depth 537.5–540.5 cm. (5–6) Cyst of *Pentapharsodinium dalei* (Indelicato and Loeblich, 1986), upper and mid foci; central body max. dia. 23 μm; sample 11A (K20/3); depth 507.5–510.5 cm. (7–8) Protoperidiniacean cyst, upper and low foci; max. dia. 44 μm; sample 9A (N43/3); depth 537.5–540.5 cm. (9–12) *Radiosperma corbiferum* Meunier, 1910 (=Sternhaar-statoplast of Hensen, 1887), upper (9–10), mid (11) and low (12) foci; central body max. dia. 38 μm; sample 9A (M10/0); depth 537.5–540.5 cm. (13–20) *Lingulodinium machaerophorum* (Deflandre and Cookson, 1955). (13–16) Specimen with processes of normal length (8–10 μm); upper (13–14), mid (15) and low (16) foci; central body max. dia. 51 μm; sample 9A (F35/4); depth 537.5–540.5 cm. (17–20) Specimen with bulbous processes; upper (17–18) and mid (19–20) foci; central body max. dia. 46 μm; sample 9A (J51/0); depth 537.5–540.5 cm.

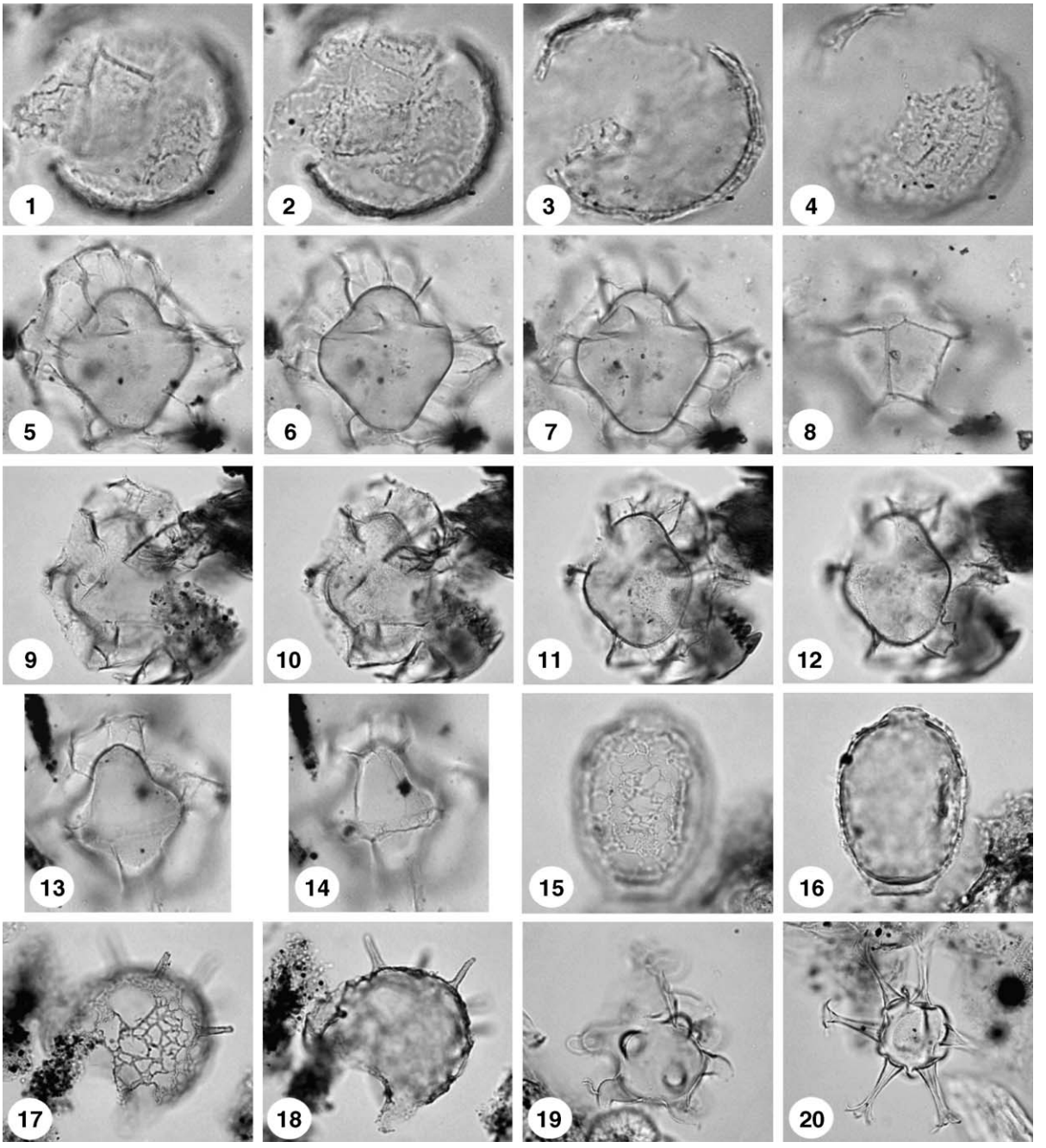

Fig. 7. Dinoflagellate cysts and other aquatic palynomorphs from Chernyshov Bay. Light micrographs in bright-field. An England Finder reference is given after the sample number. (1–4) *Caspidinium rugosum* Marret, 2004. Upper (1–2), mid (3) and low (4) foci; central body max. dia. 52 μm; sample 32A3; depth 607.5–610 cm. (5–8) *Spiniferites cruciformis* Wall et al., 1973, ventral view showing ventral surface (5), mid focus (6–7) and dorsal surface (8); sample 32A3; central body max. dia. 52 μm; depth 587.5–590 cm. (9–12) *S. cruciformis* Wall et al., 1973, ventral view showing ventral surface (9–10), mid focus (11) and dorsal surface (12); central body length 51 μm; sample 9A (J25/0); depth 537.5–540.5 cm. (13–14) *S. cruciformis* Wall et al., 1973, low focus (13) and slightly lower focus of the dorsal surface in ventral view (14) showing archeopyle; central body max. dia. 51 μm; sample 32A3; depth 547.5–550.5 cm. (15–16) Tintinniid? lorica, upper (15) and mid (16) foci; total length 53 μm; sample 1A (P27/0); depth 457.5–459.5 cm. (17–18) Incertae sedis 1, upper (17) and mid (18) foci; central body maximum diameter 77 μm; sample 1A (P27/0); depth 457.5–459.5 cm. (19) Incertae sedis 2, upper focus; total length 62 μm; sample 9A (M10/0); depth 537.5–540.5 cm. (20) *Hexasterias problematica* Cleve, 1900, mid-focus; central body max. dia. 38 μm; sample 11A (J31/3); depth 507.5–510.5 cm.

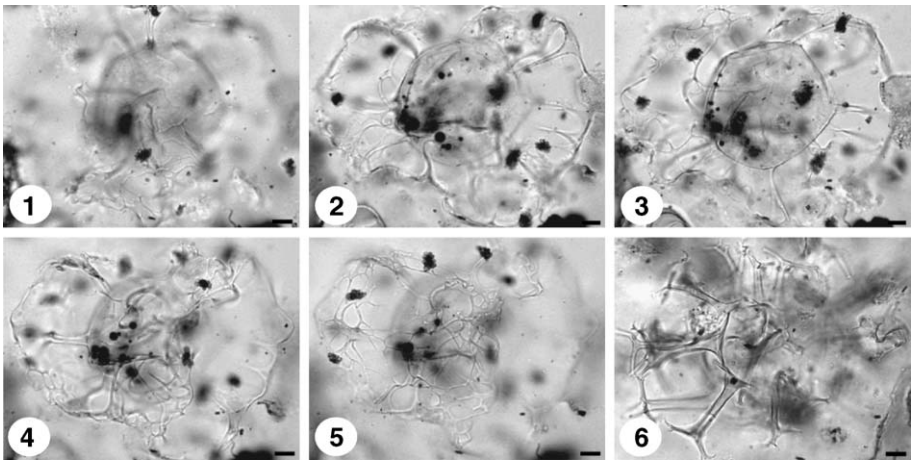

Fig. 8. Dinoflagellate cysts from Chernyshov Bay. Light micrographs in bright-field. (1–5) *Romanodinium areolatum* Baltes, 1971b, upper (1–2), mid (3) and lower (4–5) foci; central body max. dia. 63 μm; sample 32A3; depth 587.5–590 cm. (6) Reworked specimen of *Spiniferites validus* Süto-Szentai, 1982 low focus; central body max. dia. 71 μm sample 32A3; depth 607.5–610 cm.

biased by concentration values, a principal component analysis was performed on selected variables using the software "Past". The results revealed that no relevant link exists between the different variables.

2.4. Ecological groupings of dinoflagellate cysts and other palynomorphs

The in-situ dinoflagellate cyst flora is of low diversity and comprises the following taxa: *Impagidinium caspienense* (Fig. 6.1–6.4), cysts of *Pentapharsodinium dalei* (Fig. 6.5–6.6), protoperidiniacean cysts (Fig. 6.7–6.8), *Lingulodinium machaerophorum* (Figs. 6.13–6.20 and 9), *Caspidinium rugosum* (Figs. 7.1–7.4 and 10.1–10.3), *Spiniferites cruciformis* (Figs. 7.5–7.8 and 10.4–10.7) and morphotypes assigned to *Romanodinium areolatum* (Fig. 8.1–8.5). The species are grouped according to their ecological preferences. Additional aquatic palynomorph taxa recorded are specimens of the chlorophycean (green algal) taxon *Botryococcus braunii*-type (Fig. 10.9) and *Pediastrum* sp.; the prasinophycean (green flagellate) species *Hexasterias* (al. *Polyasterias*) *problematica* (Fig. 7.20) and genus *Cymatiosphaera*; loricae of the ciliate order Tintinniida (Fig. 7.15–7.16); and incertae sedis taxa including *Micrhystridium* (a probable algal cyst), Incertae sedis sp. 1 (Fig. 7.17–7.18), Incertae sedis sp. 2 (Fig. 7.19) and *Radiosperma corbiferum* (Figs. 6.9–6.12 and 10.9).

- *L. machaerophorum* (Figs. 6.13–6.20 and 9) is a euryhaline species that can tolerate salinities as low as about 10–15 g kg^{-1} (see Head et al., 2005, pp. 24–25 for review) and as high as about 40 g kg^{-1} based on laboratory culturing studies (Lewis and Hallett, 1997), or indeed higher than 40 g kg^{-1} and approaching 50 g kg^{-1} as indicated by its distribution in surface sediments of the Persian Gulf (Bradford and Wall, 1984). The motile stage of this species blooms in late summer, and has a tropical to temperate distribution, with a late-summer minimum temperature limit of about 10–12 °C (Dale, 1996; Lewis and Hallett, 1997). Since *L. machaerophorum* develops different morphotypes with respect to changing temperature (−3 to 29 °C) and salinity of surface-waters, it is regarded as a reliable indicator of environmental changes in a water body. These morphotypes are characterized by large variations in process length and shape (Fig. 4). Up to 15 different process types have been found for *L. machaerophorum* in previous studies (Wall et al., 1973; Harland, 1977; Kokinos and Anderson, 1995; Lewis and Hallett, 1997; Hallett, 1999). Most of these process types are also found in the late Holocene sediments of Chernyshov Bay. Typical specimens (Figs. 6.13–6.16 and 9.7–9.8) have processes of moderate length (5–15 μm) that taper distally to points, while other specimens may have long processes (15–20 μm; Fig. 9.1–9.3) again tapering to points and often bearing small spinules at their distal ends. Some specimens with long, curved processes are also seen. Specimens with reduced processes (≤5 μm; Fig. 9.4–9.6) are found with terminations that are columnar, pointed or bulbous (Figs. 6.17–6.20 and 9.9).
- *P. dalei* (Fig. 6.5–6.6) is a spring-blooming species (Dale, 2001) most common in high northern latitudes (Rochon et al., 1999; de Vernal et al., 2001; Marret and Zonneveld, 2003). It tolerates a wide

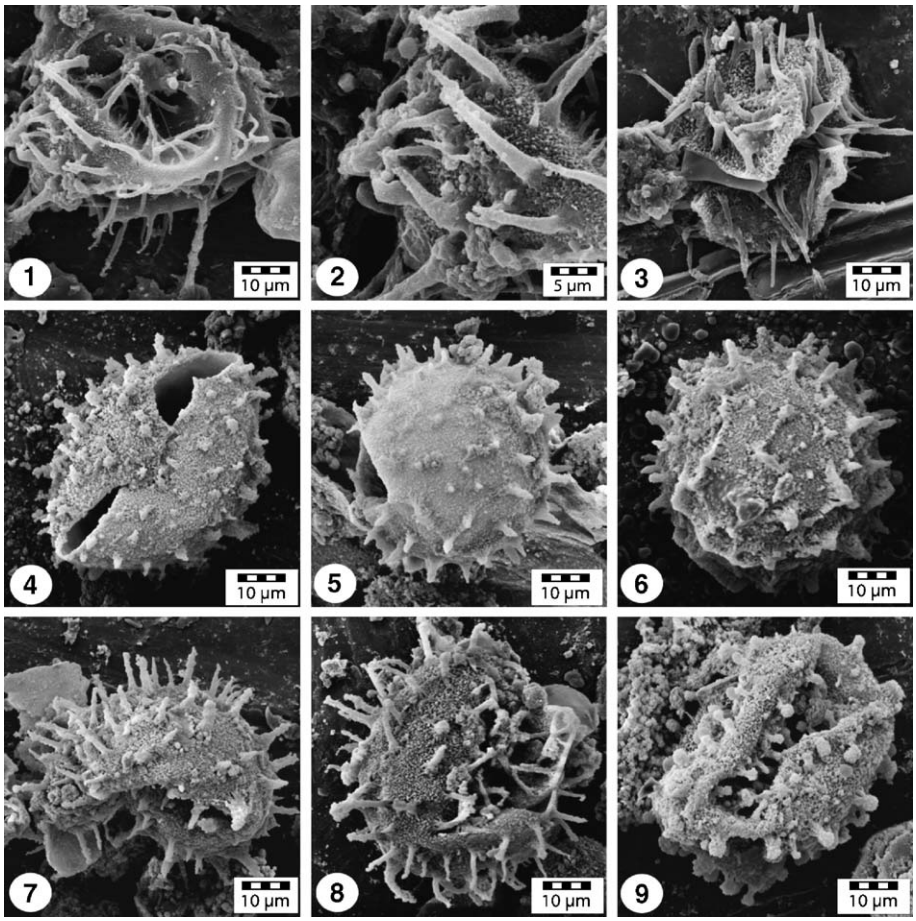

Fig. 9. Morphotypes of *Lingulodinium machaerophorum* from Chernyshov Bay. Scanning electron micrographs. (1–3) *L. machaerophorum* with long processes; sample 11A; depth 507.5–510.5 cm. (4–6) *L. machaerophorum* with reduced processes; sample 11A; depth 507.5–510.5 cm. (7–8) *L. machaerophorum* with processes of normal length; sample 11A; depth 507.5–510.5 cm. (9) *L. machaerophorum* with bulbous processes; sample 11A; depth 507.5–510.5 cm.

range of salinities (21–37 g kg^{-1}) and nutrient concentrations judging from a literature compilation of its cyst distribution (Marret and Zonneveld, 2003), although the small size and inconspicuous morphology of these cysts suggest the possibility of misidentification. Its presence in the Aral Sea core may be related to cool spring surface-waters resulting from cold winters (<0 °C).

- *S. cruciformis* (Figs. 7.5–7.14 and 10.4–10.7) in our section shows similar morphological variability to that described from the Holocene of the Black Sea by Wall et al. (1973) and Wall and Dale (1974), and as that described for modern and submodern specimens of the Caspian Sea (morphotypes A, B and C; Marret et al., 2004). *S. cruciformis* was first described from Late Pleistocene to early Holocene (23 to 7 ky BP) sediments from the Black Sea (Wall et al., 1973). The ecological affinities of *S. cruciformis* have already been discussed in several papers because this species has been found in other Eurasian water bodies, such as the Black, Marmara and Aegean seas (Aksu et al., 1995a,b; Mudie et al., 1998, 2001, 2002; Popescu, 2001), and the Caspian Sea (Marret et al., 2004), but also in Lake Kastoria sediments of Late Glacial and Holocene ages (Kouli et al., 2001). Its occurrence was also reported from Upper Miocene/Lower Pliocene sediments of the Paratethys (Popescu, 2001; Popescu, in press) and Mediterranean realms (Kloosterboer-van Hoeve et al., 2001). The shape and size of sutural septa, ridges and processes have been all described as extremely variable (Wall et al., 1973; Mudie et al., 2001). Such variations may be linked to fluctuations in salinity (Dale, 1996). In this study, specimens assigned to *S. cruciformis* vary widely in body shape and degree of development of sutural septa and flanges. The size of the central body is rather

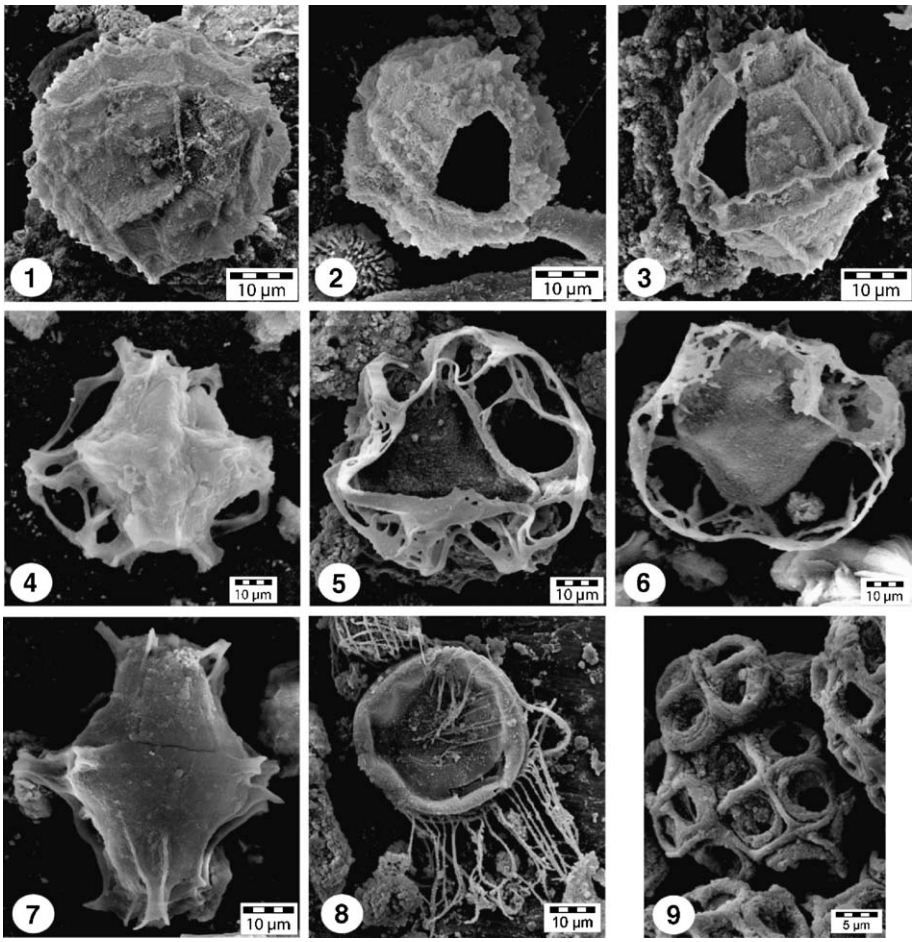

Fig. 10. Dinoflagellate cysts and other aquatic palynomorphs from Chernyshov Bay. Scanning micrographs. (1–3) *Impagidinium caspienense* Marret, 2004. Antapical view (1) and dorsal views showing archeopyle (2–3); sample 11A; depth 507.5–510.5 cm. (4–7) *Spiniferites cruciformis* Wall et al., 1973. (4) Cruciform/ellipsoidal body with a well-developed and perforated flange, ventral view; sample 24B; depth 49–51 cm. (5) Cruciform body with well-developed and perforated flange, ventral view; sample 24B; depth 4951 cm. (6) Cruciform/ellipsoidal body with well-developed and perforated flange, ventral view; sample 24B; depth 49–51 cm. (7) Cruciform body with incipient flange formed by incomplete development of low septa, dorsal view; sample 24B; depth 49–51 cm. (8) *Radiosperma corbiferum* Meunier, 1910 (=Sternhaarstatoplast of Hensen, 1887), dorsal view showing pylome; sample 11A; depth 507.5–510.5 cm. (9) *Botryococcus braunii*-type; sample 11A; depth 507.5–510.5 cm.

similar between specimens (length 40–50 µm; width 30–40 µm). The central body is either cruciform or ellipsoidal to pentagonal in shape. The degree of variation in the development of the flanges/septa consists of: (1) no development (Fig. 10.7), (2) low, fenestrate septa and incipient flange development (Fig. 10.4), or (3) well-developed and perforate–fenestrate flanges and septa (Figs. 7.5–7.14 and 10.5–10.6). However, there is a full range of intermediate variability. Specimens assignable to *R. areolatum* (Baltes, 1971a,b) are presented in Fig. 8.1–8.5. Because of the presence of morphologies intermediate between *S. cruciformis* and *R. areolatum* in our material, we have grouped these two species together in the counts (Fig. 4).

- *I. caspienense* (Figs. 6.1–6.4 and 10.1–10.3) and *C. rugosum* (Fig. 7.1–7.4) have recently been described from surface and subsurface sediments of the Caspian Sea by Marret et al. (2004). These species are apparently endemic to Central Asian Seas. However, since they might respond to different controls, they were plotted separately (Fig. 4). *I. caspienense* is the most abundant species encountered in sediments from section CH2/1, although our detailed understanding of its ecological requirements is poor. It thrives in low salinity waters (Marret et al., 2004).
- Protoperidiniacean cysts are also frequent (Fig. 6.7–6.8). These are large, smooth, spherical to subspherical pale brownish cysts, often folded, and with a rarely visible archeopyle. They are considered het-

erotrophic, and their presence may be related to elevated nutrient levels from river inflow. Because they typically feed on diatoms and other primary producers, protoperidiniacean cysts, such as those of the genus *Protoperidinium*, are regarded as paleoproductivity indicators (Dale and Gjellsa, 1993; Dale, 1996). Moreover, since they are very sensitive to post-depositional oxygen-related decay, they give crucial information on past variations in bottom water and/or pore water circulation in the sediment (Zonneveld et al., 2001). As we expect anoxic conditions (oxygen-depleted conditions) to have prevailed on the lake bottom during the time window studied (resulting from the highly stratified waters), we can therefore here use protoperidiniacean cysts as a paleoproductivity indicator.

- Freshwater algal taxa are represented by coenobia of the chlorococcalean (green algae) genus *Pediastrum*, and by colonies of the chlorococcalean *B. braunii*-type (Fig. 10.9). *Pediastrum* is a predominantly freshwater genus (Parra Barientos, 1979; Bold and Wynne, 1985), although records from brackish habitats are documented (Brenner, 2001). *Botryococcus* is mostly associated today with freshwater environments, although records from brackish habitats are also known (Batten and Grenfell, 1996). On the grounds of probability (see also Matthiessen et al., 2000), we regard *Pediastrum* and *B. braunii*-type as indicators of freshwater discharge into Chernyshov Bay.

In addition to the groups discussed above, other aquatic taxa occur in low quantities. The distributions of these taxa are listed individually in Fig. 5.

- *Radiosperma corbiferum* (Figs. 6.9–6.12 and 10.8) is a marine to brackish organism previously recorded from the living plankton of the South-Western Baltic Sea (as Sternhaarstatoblast in Hensen, 1887), Baltic Sea proper including the eastern Gulf of Finland where summer surface salinities are below 3 g kg^{-1} (Leegaard, 1920) and the Barents Sea (Meunier, 1910). It has been reported also from modern sediments of the brackish Baltic Sea where it occurs in nearly all samples from a transect representing low salinity (<6 g kg^{-1}) in the western Gulf of Finland to relatively high salinity (about 25 g kg^{-1}) in the Skagerrak (as Organismtype A in Gundersen, 1988, pl. 4, fig. 4). Highest concentrations were recorded in the central Baltic Sea where summer surface salinities are around 6–7 g kg^{-1}. Elsewhere, *R. corbiferum* has been reported from modern surface sediments of the Laptev Sea (Kunz-Pirrung, 1998, 1999), where this species has highest values north and east of the Lena delta and in front of the Yana river mouth (Kunz-Pirrung, 1999). It is also known from modern sediments of the Kiel Bight, South-Western Baltic Sea (as Sternhaarstatoblast of Hensen, 1887, in Nehring, 1994) and from sediments of Guanabara Bay at Rio de Janeiro, Brazil (Brenner, 2001). In the fossil record, *R. corbiferum* has been reported from Holocene deposits of the central Baltic Sea (Brenner, 2001) and Last Interglacial deposits of the South-Western Baltic Sea (Head et al., 2005). This distinctive but biologically enigmatic organism evidently has a broad salinity tolerance and, although it has been reported mostly from brackish-marine environments, factors additional to salinity may also control its distribution (Brenner, 2001).
- *Hexasterias* (al. *Polyasterias*) *problematica* (Fig. 7.20) has been recorded previously from Baffin Bay fjords where it is one of several species that increase towards the meltwater plumes (Mudie, 1992). It has also been found in modern sediments of the Laptev Sea (Kunz-Pirrung, 1998, 1999) and the plankton of the North Sea region (Cleve, 1900) as well as in the same general area (as "Röhrenstatoblast" in Hensen, 1887). It appears to be a brackish or euryhaline species (Matthiessen et al., 2000).
- The other aquatic groups (Fig. 7.15–7.16 and 7.17–7.18) here identified have either broad or uncertain environmental preferences.

Reworked specimens were found to occur generally within intervals of increased freshwater inflow. One group includes *Charlesdownia coleothrypta*, *Enneadocysta arcuata*, *Deflandrea phosphoritica*, *Phthanoperidinium comatum*, *Dapsilidinium pseudocolligerum*, *Areosphaeridium diktyoplokum*, and *Spiniferites* spp. (Fig. 8.6), and represents Palaeogene reworking. These specimens are often distinguished by an increased absorption of safranin-o stain, which probably reflects the oxidation history of these reworked specimens. A second group of reworked taxa, notably *Spiniferites* cf. *falcipedius*, *S. bentorii* (a single specimen), *S. hyperacanthus*, *S. membranaceous*, *S. ramosus*, *S. bulloideus*, *Spiniferites* sp., *Operculodinium centrocarpum* sensu Wall and Dale, 1966, is characterized by thin-walled cysts generally not affected by the safranin-o stain. Most of these specimens (*Spiniferites* cf. *falcipedius*, *S. bentorii*, *S. hyperacanthus*, *O. centrocarpum* sensu Wall and Dale, 1966) represent a typical Mediterranean assemblage that occurs in peak frequencies when river transport is implicated. We therefore

presume that they have been reworked from upper Neogene or Quaternary deposits, and their presence is probably linked to Plio-Pleistocene connections between the Aral, Caspian, Black and Mediterranean seas.

3. Results

Seven ecostratigraphic zones have been distinguished by statistically assessing major changes in the composition of the dinoflagellate cyst assemblage (Figs. 4 and 5). These ecostratigraphic zones mostly coincide with the lithological units previously defined.

Zone DC-a (10.75–9.97 m) is characterized by the dominance of *L. machaerophorum* as a whole, with maximum total values of 63% at 10.16 cm. Morphotypes bearing short- and normal-length processes are abundant (respectively up to 29% and 21% at 10.06 m) while specimens with long and bulbous processes are present (respectively up to 6% and 8% at 10.16 m). Frequencies of protoperidiniacean cysts fluctuate at relatively high numbers and oscillate between 18% at 9.97 m and 70% at 10.36 m. Note the reciprocating fluctuations in the frequencies of *L. machaerophorum* and protoperidiniacean cysts. Counts of *B. braunii*-type depict a somewhat decreasing trend through this zone, with relative abundances of 75% at 10.66 m to 57% at 9.97 m, as do numbers of *Pediastrum*, decreasing from 10.6% at 10.75 m to 1.7% at 9.97 m. Abundances of *I. caspienense* are relatively low throughout this zone where they average 10%, when frequencies in cysts of *P. dalei* display maximum values of 18% at 10.75 m. Reworked taxa are also present in low abundances, amounting to 20% at 10.75 m. Preservation is good throughout this zone and the dinoflagellate cyst concentration is relatively low (300–1300 specimens g^{-1}). The abrupt shift that characterizes the upper limit of this zone at 9.97 cm is related not to natural causes but to a coring failure.

Zone DC-b (9.97–6.18 m) is dominated by the species *I. caspienense*, which averages 70% to 80% for most of the zone. The previously dominant species *L. machaerophorum* disappears almost totally at the base, but occurs discretely again upwards (10% in total at 6.22 m). Counts of protoperidiniacean cysts are relatively constant throughout this zone (10–20%) but nevertheless exhibit a marked increase around 7.13 m (41%). Freshwater taxa, as well as cysts of *P. dalei*, are present as well, the latter increasing in abundances from the lower part to the top, attaining 15% at 6.18 m. Low abundances of *C. rugosum* (up to 2%) are also recorded. Dinoflagellate cyst concentrations are medium (500–7250 cysts g^{-1}) and the preservation is poor due to crumpling of cysts.

Zone DC-c (6.18–4.64 m) documents the co-occurrence of two dominant taxa: *L. machaerophorum* and *I. caspienense*. While *I. caspienense* values remain relatively constant throughout this interval (50–60% on average), relative abundances of *L. machaerophorum* depict a progressive increase from 14% at bottom up to 91% at 4.64 m in total (respectively minimal and maximal values of 0–30%, 0–6%, 0–41.5% and 0–8% from morphotypes with normal length, long, short and bulbous processes). Conversely, relative abundances of protoperidiniacean cysts decrease from 27% at 6.09 m to 2% at 4.71 cm (0% at 5.14 m). Also, cysts of *P. dalei* (0–5%) and freshwater taxa (<10% on average but 40% at 4.695 m) occur in low numbers throughout this zone. *S. cruciformis* including *R. areolatum* is mostly found in the lowermost part (between 5.99 and 5.69 m; 1–2%) although they also occur in low frequencies near the top. *C. rugosum* is rare (up to 1.5%). Preservation is very good in this zone; correlatively the dinoflagellate cyst concentration is relatively high (from 800 to ca. 22,000 cysts g^{-1}; Fig. 5). There is also a noticeable increase in the concentration of *Michrystridium braunii*-type organisms throughout this zone (up to ca. 12,000 specimens g^{-1} at the top). The transition from Zone DC-c to DC-d coincides with the transition from lithological Unit 2 to 3 (Fig. 2).

Zone DC-d (4.64–2.62 m) is characterized by an abrupt increase in the relative abundance of protoperidiniacean cysts, with a maximum of 95.8% at 3.18 m and frequencies fluctuating around 70% between 3.95 m and 2.72 m. Correspondingly, after an abrupt increase in the frequencies of freshwater species (notably *B. braunii*-type) with average values increasing up to 96.5% at 4.59 m, the abundance shows a progressive decreasing trend upwards (18% at 2.62 m). Abundances of reworked dinoflagellate cysts are also high in this zone, increasing to 75% at 3.75 m and at 3.58 m, before progressively decreasing further upwards. Abundances of *L. machaerophorum* show a stepwise decrease from 91% at 4.64 m (ecozonal boundary Zones DC-c/d) to 1% at 2.72 m. Relative abundances of cysts of *P. dalei* remain very low (<5%) in this zone. *S. cruciformis* including *R. areolatum* is found in low abundances (1–3%), mostly between 3.08 and 2.62 m. Also present are reworked specimens of *Spiniferites* species, including *S. ramosus* and *S. bulloideus*, which occur as smooth, thin-walled and delicate specimens. This zone is characterized by very low concentrations of dinoflagellate cysts (30–600 specimens g^{-1}) and poor preservation.

Zone DC-e (2.62–0.5 m) is characterized by the replacement of protoperidiniacean cysts (20% on average but 4% at 2.32 m) by *I. caspienense* that becomes conspicuously dominant, with average values amounting to 60%. Correspondingly, relative abundances of reworked taxa significantly decline (ca. 20% at 2.62 m to 8% at 0.6 m). Frequencies of *L. machaerophorum* are low throughout this zone, although a slight increase is noticeable between 1.36 m and 1.05 m (10–20%). *S. cruciformis* including *R. areolatum* is more scarcely represented in this zone with contributions never exceeding 2% of the dinoflagellate cyst assemblage. Relative abundances of cysts of *P. dalei* are relatively constant (~5%) but conspicuously increase at the top (16% at 0.5 m). Rare cysts of *C. rugosum* are also present (1–3%). Dinoflagellate cyst concentrations are again low (70 to 800 specimens g^{-1}) although the preservation is much better.

Zone DC-f (0.5–0 m) is characterized by the dominance of *L. machaerophorum* morphotypes whose relative abundances abruptly increase from 0.5 m upwards (normal length processes: 20%; long processes: 10%; short processes: 30%; bulbous processes: 1% at the very top). Conversely, relative abundances of *I. caspienense*, protoperidiniacean cysts and morphotypes of *S. cruciformis* noticeably decrease between 0.5 m and the topmost part of this zone, with respective values of 16% at 0.5 m to 8% at 0 m for *I. caspienense*, 68% to 23% for the protoperidiniacean cysts and 21% to 7% for the morphotypes of *S. cruciformis*. Cysts of *P. dalei* progressively disappear with values ranging from 16% at 0.5 m to 0% at the top. Dinoflagellate cyst preservation is very good throughout this zone but the concentration remains relatively low (200–8000 cysts g^{-1}).

4. Discussion

4.1. Palaeoenvironmental reconstruction

For the past 2000 years, two contrasting environmental states can be distinguished, each with distinct extremes. Transiently highly saline (poly- to meta-/hypersaline) conditions are inferred by specific dinoflagellate cyst assemblages characterized by increasing/high abundances of *L. machaerophorum*. Coevally, gypsum starts to precipitate from the water column as soon as the salinity reaches 28 g kg^{-1} (Brodskaya, 1952; Bortnik and Chistyaeva, 1990). Since the motile stage of *L. machaerophorum* commonly blooms in late summer, persistently higher abundances of this species may imply sustained levels of enhanced evaporation. Conversely, periods of decreasing salinity (oligo-/meso-saline conditions: 0.5–25 g kg^{-1}) are inferred from dinoflagellate cyst assemblages characterized by decreasing frequencies of *L. machaerophorum* (and reduced processes: <5 μm) but increased abundances of other autotrophic (notably *I. caspiniense*) and heterotrophic (protoperidiniacean cysts) species. Higher abundances of freshwater algae (*Pediastrum*, *B. braunii*-type) imply river discharge and periods of freshening of the lake. Furthermore, due to its ecological preferences, *P. dalei* may serve as a proxy for cool spring surface-waters following cold winters. The dinoflagellate cyst record can thus be used to infer surface-water variations in salinity, palaeoproductivity and potentially also temperature. Because these changes imply fluctuations in lake water level, coeval changes in sedimentation and environmental processes should have occurred. The palaeoenvionmental changes are discussed here in terms of contrasting environmental states, notably salinity and lake water levels (see Fig. 4).

Today, salt concentrations in the Western Basin have increased to 82 g kg^{-1} in surface-waters and 110 g kg^{-1} at depth (Friedrich and Oberhänsli, 2004). This is reflected in the topmost sediment of section CH2/1 by an abrupt increase in abundance of the autotrophic species *L. machaerophorum* (especially morphotypes with long, i.e. >15 μm and normal length, i.e. 5–15 μm, processes; Zone DC-f) within a trend strengthened at the very top. Based on this observation and the aforementioned ecological tolerances of the species, we confirm *L. machaerophorum* as a reliable environmental indicator indicating salinity increase in surface-water layers. It must be understood, however, that the motile stage of *L. machaerophorum* blooms mostly in late summer (Lewis and Hallett, 1997) and its cyst record therefore does not necessarily reflect conditions at other times of the year.

4.1.1. Zone DC-a (10.75–9.97 m: 100? BC–425 AD)

This zone is interpreted as representing a period of low lake level due to evaporative drawdown, indicated by high levels of *L. machaerophorum* and deposition of gypsum (G_1). In the Aral Sea, gypsum precipitates out in the water column once salinity attains 28 g kg^{-1} (Brodskaya, 1952; Bortnik and Chistyaeva, 1990), which thus suggests that surface water salinity during Zone DC-a was above 28 g kg^{-1}. This is in agreement with the salinity tolerance of *L. machaerophorum*, a species grown in the laboratory in salinities up to 40 g kg^{-1} (Lewis and Hallett, 1997; Hallett, 1999) and whose modern distribution in surface sediments of the Gulf of Persia implies a tolerance to salinities exceeding 40 g kg^{-1} and indeed approaching 50 g kg^{-1} (Bradford

and Wall, 1984). *L. machaerophorum* blooms in late summer, and high numbers indicate sustained periods of enhanced summer evaporation during Zone DC-a. At the same time, abundant fresh-water algae *B. braunii*-type and *Pediastrum* sp., and nutrient-dependent (protoperidiniacean) cysts, also characterise this zone and indicate freshwater inflow and increased palaeoproductivity. The source of the freshwater inflows remains debatable. These episodic freshwater influxes are possibly linked to phases of stronger discharges of the Syr Darya and Amu Darya rivers in late spring/early summer. They can also originate from local rivers episodically flushing into the bay (Fig. 1), such as the Irgiz River in the north (see Aleshinskaya et al., 1996). The seasonal contrast in sea-surface temperatures, when judging from significant numbers of cysts of the spring-blooming, cool-tolerant species *P. dalei*, was probably higher between 100? BC and 425 AD, with relatively cool spring surface-water temperatures following cold winters.

4.1.2. Zone DC-b (9.97–6.18 m: 425–920 AD)

I. caspienense is a brackish species judging from its modern distribution in the Caspian Sea, although it overlaps ecologically with *L. machaerophorum* in the lower range of the latter species' salinity tolerance (Marret et al., 2004). The dominance of *I. caspienense* in this zone and near absence of *L. machaerophorum* indicates that the surface water salinity was below 15 g kg^{-1} and probably around 10 g kg^{-1} (the approximate lower limit for *L. machaerophorum*). The presence of *P. dalei* and protoperidiniacean cysts is not inconsistent with this interpretation, as these species are present in the low-salinity Caspian Sea today (Marret et al., 2004). The reduction in salinity during Zone DC-b implies that the lake level had risen substantially (although we do not know if this was gradual or abrupt because of the coring break). Because of the low topography of the shorelines around the lake, even a slight rise in lake level will have a substantial effect on the position of the shoreline. It will have expanded outwards considerably in all directions, and will have moved substantially away from the coring site. This may explain why Zone DC-b has low representations of *B. braunii*-type and *Pediastrum* sp.—the river discharges supplying these allochthonous palynomorphs being further away.

4.1.3. Zone DC-c (6.18–4.64 m: 920–1230 AD)

A relatively steady increase in *L. machaerophorum* and reciprocal decrease in the brackish species *I. caspienense* together evidences a progressive salinity increase in this zone, with precipitation of gypsum (G_2) near the top. A pronounced increase in dinoflagellate cyst concentration within this zone probably signifies increased productivity as a response to the rise in salinity. Judging from the presence of gypsum deposits and tolerance of *L. machaerophorum* to high salinities, it would seem that salinities rose above 28 g kg^{-1}. The increasing salinity throughout this zone suggests progressive lowering of the lake level.

4.1.4. Zone DC-d (4.64–2.62 m: 1230–1400 AD)

This zone represents a progressive decline in salinity, as evidenced by a reduction in *L. machaerophorum* to near disappearance at the top of the zone. This was evidently caused by freshwater inflow into the lake, as indicated by abundant *B. braunii*-type. This zone is also characterized by a drastic change in sedimentation from the deposition of laminated sediments to silty clays (Fig. 2) rather poor in palynomorphs (Fig. 5). The coring site was clearly receiving significant river discharges because reworked cysts are also abundant. These reworked cysts attest to active erosion of Neogene and late Quaternary deposits during periods of elevated sheet-wash from shore, and account for the high sediment accumulation rates in this zone (16 mm $year^{-1}$, see also Nourgaliev et al., 2003). Nutrient input at this time is reflected in the high levels of protoperidiniacean cysts. However, general productivity is likely to have been lower in this zone than Zone DC-c because of the declining salinity. The low values of *I. caspienense* seem to be caused by reciprocally high values of protoperidiniacean cysts. The progressive decline in both *B. braunii*-type and reworked cysts probably relates to the expansion of the lake as it continued to fill, which will have caused rivers supplying freshwater to the lake to recede from the core site. Judging from low numbers of the cool-tolerant species *P. dalei*, spring surface-water temperatures were probably higher between 1230 AD and 1400 AD, implying relatively mild winters.

4.1.5. Zone DC-e (2.62–0.5 m: 1400–1800 AD)

The lower part of this zone represents a continuance of reduced salinities established at the top of Zone DC-d, marked by low levels of *L. machaerophorum* and high levels of *I. caspienense*. Conditions were comparable to those in DC-b, with salinity probably around 10–15 g kg^{-1} or slightly less. The abrupt decline in protoperidiniacean cysts (causing a reciprocally abrupt increase in *I. caspienense*) might be explained in terms of a gradual lowering of salinity that abruptly exceeded the physiological limit of the protoperidiniaceans. Salinities were evidently increas-

ing through the lower part of Zone DC-e (1500 and 1600–1650 AD), as evidenced by increased values of *L. machaerophorum* and declining values of *I. caspienense*. This seems to have culminated in the gypsum layer G_3 in the middle of the zone. The upper part of Zone DC-e is more difficult to reconstruct but salinities were certainly above 10 g kg^{-1}, judging from the persistence of *L. machaerophorum*, yet remained brackish given the high values of *I. caspienense*.

4.1.6. Zone DC-f (0.5–0 m: 1800–1980 AD)

A return to progressively more saline conditions, as prevails today, is evidenced by an increase in *L. machaerophorum*, reduced levels of *I. caspienense*, and the formation of gypsum (G_4) within this zone. Also cooler spring surface-water temperatures following harsher winter conditions are reflected by higher abundances of cysts of *P. dalei* around 1900 AD.

4.2. Palaeoclimatic changes inferred from dinoflagellate cysts

Numerous previous studies indicate that climates of the Central Asian deserts and semi-deserts have experienced different changes from hyper-arid deserts to more humid semi-arid conditions at various temporal scales during the late Quaternary and Holocene (e.g. Tarasov et al., 1998; Velichko, 1989). During the past few thousand years these changes have resulted in multiple lake level changes (e.g. Létolle and Mainguet, 1993; Boomer et al., 2000; Boroffka et al., 2005). The present-day climate in western Central Asia is mainly controlled by the Westwind Drift carrying moist air to the mountain ranges which condenses as snow in the Pamir and Tien-Shan, the catchment areas of the two tributaries feeding the Aral Sea. Thus the meltwater discharged by Syr Darya and Amu Darya rivers largely controls the hydrological balance in the lake during late spring and early summer. In addition, local precipitation occurs during late winter and early spring when depressions, developing over the Eastern Mediterranean, subsequently move along a northeast trajectory where they may even replenish moisture over the Caspian Sea (Lioubimtseva, 2002). This adds to the water balance in the Aral Sea. Hence the relative abundance of reworked dinoflagellate cysts is expected to increase during periods of elevated sheet-wash from shore caused by enhanced moisture derived from the Mediterranean Sea. A third factor of importance, though difficult to quantify is the seasonally changing evaporation rate probably due to short-term changes in solar insolation. During the past few thousand years these factors have exerted control on the water balance to varying degrees.

The dinoflagellate cyst record indicates prominent salinity increases during the intervals ca. 0–425 AD (or 100? BC–425 AD), 920–1230 AD, 1500 AD, 1600–1650 AD, 1800 AD and the modern increase (Fig. 11). The lowermost sequence (Zone DC-a, Unit 4), which represents the first few centuries AD, characterizes as a whole elevated salinity levels resulting in gypsum precipitation (G_1) during an important phase of lake level lowering (27–28 m a.s.l.; see Nurtaev, 2004). During this time period, salinity increases mainly occurred at around 0 AD, 100–200 AD and 350–425 AD, probably resulting from considerably lowered meltwater run-off supplied by the rivers due to lowered late spring and summer temperatures in the mountains of the high altitude catchment. This is contemporaneous with glacier expansion during 2100–1700 yr BP in the northern and western Tien Shan (Savoskul and Solomina, 1996) and in the Pamir-Alay mountains (Zech et al., 2000). Coevally, at approximately 2000 years BP, a lake level recession is reported from Lake Van (Turkey) based on detailed palaeoclimatological studies (Landmann et al., 1996; Lemcke and Sturm, 1996) that demonstrate a period of decreasing humidity beginning at about 3500 and culminating at 2000 years BP. Similarly in Syria (Bryson, 1996) and Israel (Schilman et al., 2002), declining rainfall leading to dry events is also reported at around 2000 years BP. The decrease of rainfall is possibly related to a waning of the low-pressure system that developed over the Eastern Mediterranean and/or to a shift of the trajectories bringing moist air from the Eastern Mediterranean to the Middle East and Western Central Asia. In the Aral Sea hinterland, low levels of rainfall are inferred from low abundances of reworked dinocysts hence suggesting reduced on-land sheet-wash too.

The causes driving the progressive increase in salinity at ca. 920–1230 AD (Middle Ages) may be climatically controlled as well. The increase in salinity is accompanied by a progressive and extensive lake-level fall of the Aral Sea, as a pronounced regression was also recorded in Tschebas Bay (Wünnemann et al., submitted for publication), thus reflecting long-term declining discharges from the Syr Darya and the Amu Darya rivers around 1200 AD. These results are fairly consistent with the tree-ring width record of Esper et al. (2002) (Fig. 11) and Mukhamedshin (1977), where several short-lasting events can be correlated with our salinity curve (Fig. 11). These authors report a notable decrease in ring width from 800 AD to 1250 AD, corresponding to a colder phase in the Tien Shan and

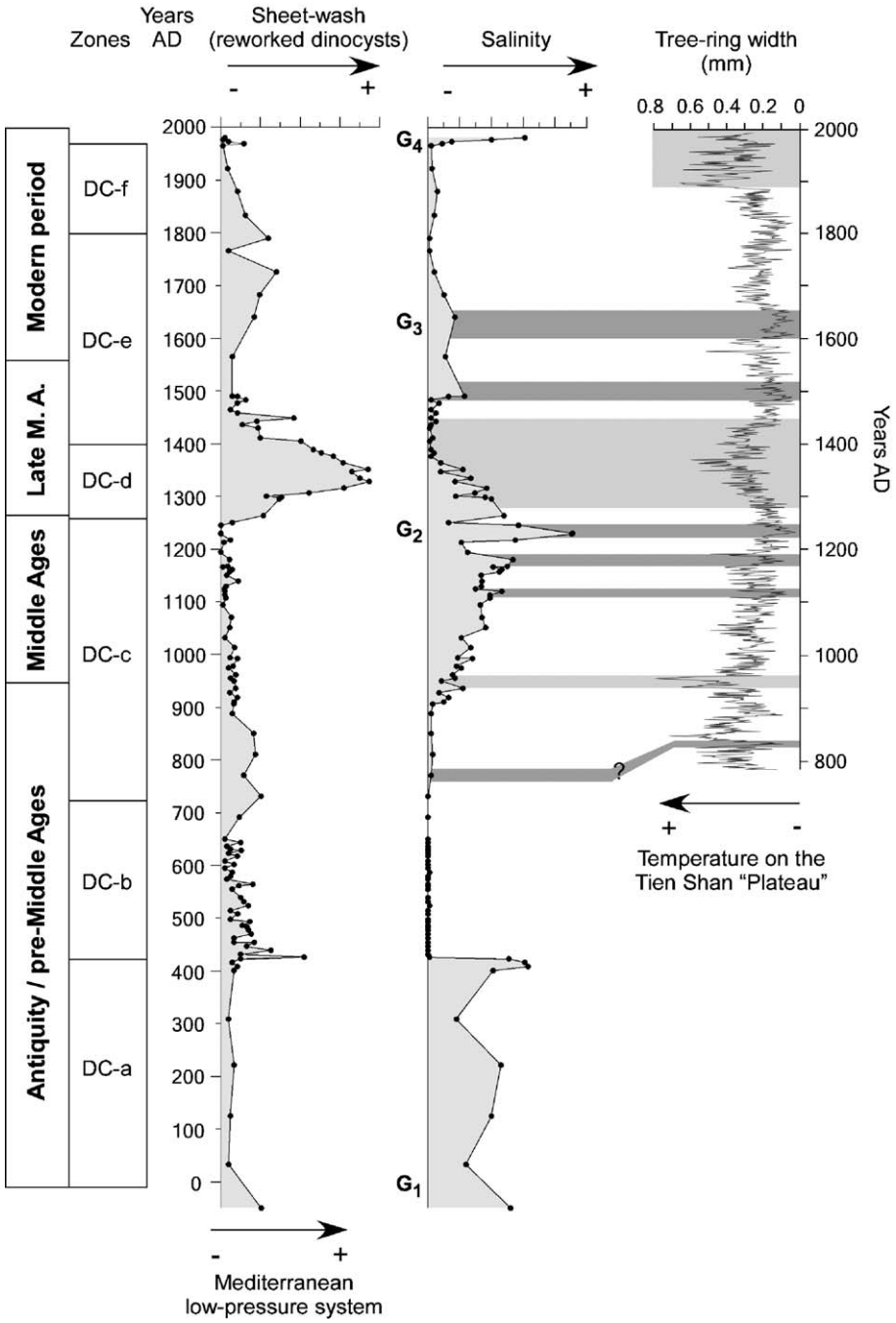

Fig. 11. Correlation of palaeoenvironmental changes during the last 2000 years as inferred from section CH2/1 with the tree-ring width record of Esper et al. (2002). The salinity reconstruction is estimated from the relative abundance of *L. machaerophorum*. Data are plotted according to the age model as detailed in Section 2.2 (Fig. 4). G_1 to G_4 refer to chemical precipitates of gypsum in section CH2/1 (see Section 2.1; Fig. 2).

Pamir-Alay mountains, respectively, with lowered late spring and summer temperatures. This is further supported by preliminary pollen analyses conducted on section CH2/1, which reflects cool and arid conditions in the Aral Sea Basin after 1000 AD. This aridification of the climate matches relatively well with variations observed in the western Tibetan Plateau by Bao et al. (2003). From air-temperature reconstructions, these authors report warming conditions during the intervals 800–1050 AD and 1250–1400 AD (Medieval Warm/

Wet Period) with a short colder phase during ca. 1050–1250 AD, and especially at around 1200 AD. The salinity increase intervening between 920 AD and 1230 AD in our record is accompanied by very low abundances of reworked dinoflagellate cysts (Fig. 11) suggesting again considerably reduced sheet-wash from the shore and thus lowered moisture derived from the Eastern Mediterranean region during the late winter and early spring seasons. This is well-supported through palaeoenvironmental records from the Eastern Mediterranean Sea (Issar et al., 1990; Schilman et al., 2002) that document colder conditions resulting in a decrease of evaporation and reduced rainfall as inferred from $\delta^{18}O$ variations of pelagic foraminifera and carbonate cave deposits (Soreq cave, Israel).

A progressive decrease in salinity (oligo-/mesosaline conditions) and a return to higher lake levels characterize the period 1230–1450 AD. Coevally, tree-ring width conspicuously increased, growing at similar rates during ca. 1360–1370 AD to those observed for the last 100 years (Esper et al., 2002). This is further confirmed by Kotlyakov et al. (1991) who reported a warming phase between the 11th and 14th–15th centuries, based on tree-ring data from the Tien Shan. Increased growing rates thus characterize higher temperatures in the mountains that result in elevated meltwater discharges to the Aral Sea in late spring/early summer. Moreover, higher abundances of reworked dinoflagellate cysts of Neogene/late Quaternary ages reflect enhanced regional spring precipitation in Central Asia from 1230–1400 AD. They document the intensified erosion of shore sediments which occurred frequently during extreme sheet-wash events linked to intensified low pressure systems over the Eastern Mediterranean. The latter is confirmed by Schilman et al. (2002) who documented higher rainfall over Israel between 1250 AD and 1500 AD.

Similarly, the two slight increases in salinity as recorded at ca. 1500 AD and 1600–1650 AD from the dinoflagellate cysts are probably climatically driven as well. The interval from 1500 to ca. 1650 AD includes the coldest decades according to the mean annual temperature reconstruction for the Northern Hemisphere (Bradley, 2000). New archaeological findings from the south Aral Sea (Boroffka et al., 2005; Shirinov et al., 2004) indicate that the lake level lowered to as much as 31 m a.s.l. at that time. A similar brief drying event has been reported at about 1650 AD by Boomer et al. (2003) from their studies on ostracods. Besides, these events are well-constrained with other records from Central Asia. Two successive decreases in tree-ring width are reported from Esper et al. (2002) between 1500 AD and 1600–1650 AD. These events match well with two salinity increases in the Aral Sea (Fig. 11) and reflect reduced meltwater inflow from the catchment area. This also closely matches a cooler phase from the Western Tibetan Plateau at ca. 1500–1550 AD and 1600–1650 AD when glaciers advanced on the southern Tibetan Plateau (Bao et al., 2003). We thus propose that this event widely expressed north of 35°N may correspond to a short-lived Little Ice Age signature in the Aral Sea sediments.

After 1650 AD, salinity slightly fluctuated around lower levels (oligo-/mesosaline conditions) suggesting higher lake levels up to 1900 AD, with nevertheless a short-lasting salinity increase around 1800 AD. This is again consistent with the tree-ring record for this time window (Esper et al., 2002), where climatic conditions appear relatively favourable for growth, except around 1800 AD where a decrease in the tree-ring width can be observed. Precipitation frequency, as inferred from the reworked dinoflagellate cysts, fluctuated slightly during this period, with probably higher rainfall at ca. 1650 and 1700 AD, but declined afterwards. Near to the top of section CH2/1, a strong environmental shift (Zone DC-f; Figs. 4 and 11) documents the onset of the modern lake level regression. Though this disaster is mostly due to the intensification of irrigation in the hinterland since the early 1960s, instrumental data already document a lake whose level was starting to lower in the late 1950s (Krivonogov, pers. comm., 2005).

4.3. Human influence on hydrography

Climate variability is probably the dominant factor controlling the hydrology in western Central Asia and thus the salinity in the Aral Sea, but one might expect human influence (irrigation activities) to also have exerted an important role in this densely settled region along the Silk Route during the past 2000 years. Since Early Antiquity (4th–2nd centuries BC) up to the pre-Islamic Middle Ages (4th–6th centuries AD), water from the Syr Darya and the Amu Darya rivers has been used on a large scale for irrigation, mostly in open canals (see Boroffka et al., 2005, in press). According to Létolle and Mainguet (1993), the hydraulic installations on the Amu Darya were completely destroyed after the invasion of Mongol warriors (the Huns Hephtalites) around 380–400 AD. Thus at that time the Aral Sea was reported to be cut-off from its main source of freshwater. Historical reports from Greek sources (Barthold, 1910) further indicate that

the Amu Darya discharged into the Caspian Sea during this period. However, this event may not be at the origin of the lake regression observed at ca. 2000 years BP because a time lag of almost 400 years would be implied. Instead it may have only amplified the retreat of the water body witnessed by an aridification in Central Asia. Similar considerations may be regarded concerning the period 920–1230 AD (Zone DC-c), which records the Middle Ages' regression. Although irrigation gradually declined up to the 13th century AD (Boroffka et al., 2005), historical reports document a total destruction of the hydraulic installations in the Khorezm region after Genghis Khan's invasion documented at 1221 AD (Létolle and Mainguet, 1993). This catastrophic event led again to a severing of the Amu Darya from the Aral Sea, which was reported as discharging into the Caspian Sea at that time. Nonetheless, our dinoflagellate cyst record rather reflects a gradual regressive phase which would not match with a catastrophic event resulting from the destruction of dams in the Amu Darya delta. We thus propose that the progressive lake level lowering inferred for the period 920–1230 AD is again most probably climatically driven, but that human activities might have further strengthened the lake level fall.

5. Conclusions

This is the first ecostratigraphic study using dinoflagellate cysts from the late Quaternary of the Aral Sea and has led to an improved understanding of the mechanisms that control environmental changes in the Aral Sea during the Late Holocene. It has also helped to unravel the influence of climate and anthropogenic activities on the hydrographic development of the Aral Sea during the past 2000 years. The results suggest that the successive lake level fluctuations are indeed climatically triggered, and result from different factors controlling the water balance in Central Asia, notably the Westwind Drift controlling temperatures in the montane regions, and local to regional rainfall sourced by migrating moisture from the Eastern Mediterranean Sea. Other factors may have influenced climate conditions over the Aral Sea Basin, such as variable solar activity, as suggested by Crowley (2000) based on climate-modelled simulations over the Northern Hemisphere. Testing this proposal would require higher-resolution analyses than presently undertaken. However, the degree of lake-level lowering may have been amplified by humans responding to changing environmental conditions. Irrigation systems were probably extended during periods of more arid conditions. Documentary evidence shows the existence of irrigation activities already during Early Classical Antiquity (before 0 BC) (Boroffka et al., 2005), indicating that lake water levels strongly depended on climate conditions at that time too. As to changes during the early to middle Holocene, ongoing research aims to unravel the respective impacts of climate and tectonics on the hydrology of the Aral Sea ecosystem.

Acknowledgments

The CLIMAN project is funded by the INTAS organization of the European Union (Project No. Aral 00-1030) and the German Science Foundation (DFG Project 436 RUS 111/663–OB 86/4). We are grateful for this support. We wish to thank especially Dr. Francois Demory for excellent support in the field. We acknowledge Dr. Gilles Escarguel, Dr. Jean-Jacques Cornée, Dr. Pierpaolo Zuddas and Samuel Mailliot (University Claude Bernard—Lyon 1) for valuable discussions and insights. The manuscript reviewers are also acknowledged for helping to improve the paper.

References

Aksu, A.E., Yasar, D., Mudie, P.J., 1995a. Palaeoclimatic and paleoceanographic conditions leading to development of sapropel layer S1 in the Aegean Sea. Palaeogeography, Palaeoclimatology, Palaeoecology 116, 71–101.

Aksu, A.E., Yasar, D., Mudie, P.J., Gillespie, H., 1995b. Late glacial–Holocene paleoclimatic and palaeoceanographic evolution of the Aegean Sea: micropaleontological and stable isotope evidence. Marine Geology 123, 33–59.

Aleshinskaya, Z.V., Tarasov, P.E., Harrison, S.P., 1996. Aral Sea, Kazakhstan–Uzbekistan. Lake Status Records FSU and Mongolia, p. 108–114.

Baltes, N., 1971a. Tertiary plant microfossil assemblages from the Pannonian depression (Rumania) and their paleoecology. Review of Palaeobotany and Palynology 11, 125–158.

Baltes, N., 1971b. Pliocene dinoflagellata and acritarcha in Romania. In: Farinacci, A. (Ed.), Proceedings, Second Planktonic Conference, Rome vol. 1970 (1). Edizioni Tecnoscienza, Rome, pp. 1–19.

Bao, Y., Bräuning, A., Yafeng, S., 2003. Late Holocene temperature fluctuations on the Tibetan Plateau. Quaternary Science Reviews 22, 2335–2344.

Barthold, W., 1910. Nachrichten über den Aral–See und den unteren Lauf des Amu-darja von den ältesten Zeiten bis zum XVII. Jahrhundert. Quellen und Forschungen zur Erd- und Kulturkunde vol. 2. Otto Wigand m.b.H., Leipzig.

Batten, D.J., Grenfell, H.R., 1996. Green and blue-green algae. 7D—*Botryococcus*. In: Jansonius, J., McGregor, D.C. (Eds.), Palynology: Principles and Applications vol. 1. American Association of Stratigraphic Palynologists Foundation, Dallas, Texas, pp. 205–214.

Bold, H.C., Wynne, M.J., 1985. Introduction to the Algae, (2nd edition). Prentice-Hall, Englewood Cliffs, NJ. 720 pp.

Boomer, I., Aladin, N., Plotnikov, I., Whatley, R., 2000. The palaeolimnology of the Aral Sea: a review. Quaternary Science Reviews 19, 1259–1278.

Boomer, I., Horne, D.J., Slipper, I., 2003. The use of ostracodes in palaeoenvironmental studies, or What can you do with an ostracod shell? Palaeontological Society Papers 9, 153–180.

Boroffka, N.G.O., Oberhänsli, H., Achatov, G.A., Aladin, N.V., Baipakov, K.M., Erzhanova, A., Hoernig, A., Krivonogov, S.K., Lobas, D.A., Savel'eva, T.V., Wuennemann, B., 2005. Human settlements on the northern shores of lake Aral and water level changes. Mitigation and Adaptation Strategies for Global Change 10, 71–85.

Boroffka, N.G.O., Oberhänsli, H., Sorrel, P., Reinhardt, C., Wünnemann, B., Alimov, K., Baratov, S., Rakhimov, K., Saparov, N., Shirinov, T., Krivonogov, S.K., in press. Archaeology and climate: Settlement and lake level changes at the Aral Sea. Geoarchaeology.

Bortnik, V.N., Chistyaeva, S.P. (Eds.), 1990. Hydrometeorology and hydrochemistry of the USSR seas, The Aral Sea vol. VII. Gidrometeoizdat, Leningrad. 196 pp. (in Russian).

Bradford, M.R., Wall, D.A., 1984. The distribution of Recent organic-walled dinoflagellate cysts in the Persian Gulf, Gulf of Oman, and northwestern Arabian Sea. Palaeontographica Abteilung B Paläophytologie 192, 16–84.

Bradley, R.S., 2000. 1000 years of climate change. Science 288, 1353–1354.

Brenner, W.W., 2001. Organic-walled microfossils from the central Baltic Sea, indicators of environmental change and base for ecostratigraphic correlation. Baltica 14, 40–51.

Brodskaya, I.G., 1952. Data and Processes on Sedimentary Deposits of the Aral Sea. tr. In-Ta Geol. Nauk, AN SSSR vol. 115. 140 pp. (in Russian).

Bryson, R.A., 1996. Proxy indications of Holocene winter rains in southwest Asia compared with simulated rainfall. In: Dalfes, H.N., Kukla, G., Weiss, H. (Eds.), Third Millenium BC; Climate Change and Old World Collapse, NATO ASI Series I vol. 49. Springer Verlag, pp. 465–473.

Cleve, P.T., 1900. The plankton of the North Sea, the English Channel, and the Skagerrak in 1898. Kungl. Svenska Vetenskapsakademiens Handlingar 32 (8), 1–53.

Cour, P., 1974. Nouvelles techniques de détection des flux et de retombées polliniques: étude de la sédimentation des pollens et des spores à la surface du sol. Pollen et Spores 23 (2), 247–258.

Crowley, T.J., 2000. Causes of climate change over the past 1000 years. Science 289, 270–277.

Dale, B., 1996. Dinoflagellate cyst ecology: modelling and geological applications. In: Jansonius, J., McGregor, D.C. (Eds.), Palynology: Principles and Applications vol. 3. American Association of Stratigraphic Palynologists Foundation, Dallas TX, pp. 1249–1275.

Dale, B., 2001. The sedimentary record of dinoflagellate cysts: looking back into the future of phytoplankton blooms. Scientia Marina 65 (Suppl. 2), 257–272.

Dale, B., Gjellsa, A., 1993. Dinoflagellate cysts as paleoproductivity indicators: state of the art, potential, and limits. In: Zahn, R., Pedersen, T.F., Kaminski, M.A., Labeyrie, L. (Eds.), Carbon Cycling in the Glacial Ocean: Constrains on the Ocean's Role in Global Change: Quantitative Approaches in Paleooceanography, NATO ASI Series I, Global Environmental Change. Springer, Berlin, pp. 521–537.

Deflandre, G., Cookson, I.C., 1955. Fossil microplankton from Australian Late Mesozoic and Tertiary sediments. Australian Journal of Marine and Freshwater Research 6, 242–313.

de Vernal, A., Henry, M., Matthiessen, J., Mudie, P.J., Rochon, A., Boessenkool, K.P., Eynaud, F., Grøsfjeld, K., Guiot, J., Hamel, D., Harland, R., Head, M.J., Kunz-Pirrung, M., Levac, E., Loucheur, V., Peyron, O., Pospelova, V., Radi, T., Turon, J.-L., Voronina, E., 2001. Dinoflagellate cyst assemblages as tracers of sea-surface conditions in the northern North Atlantic, Arctic and sub-Arctic seas: the new '$n=677$' data base and its application for quantitative palaeoceanographic reconstruction. Journal of Quaternary Sciences 16, 681–698.

Esper, J., Schweingruber, F.H., Winiger, M., 2002. 1300 years of climate history for Western Central Asia inferred from tree-rings. Holocene 12, 267–277.

Friedrich, J., Oberhänsli, H., 2004. Hydrochemical properties of the Aral Sea water in summer 2002. Journal of Marine Systems 47, 77–88.

Gundersen, N., 1988. En palynologisk undersøkelse av dinoflagellatcyster langs en synkende salinitetsgradient i recente sedimenter fra Østersjø-området. Cand. Scient. Dissertation, Geologisk Institutt, Universitetet i Oslo.

Hallett, R.I., 1999. Consequences of environmental change on the growth and morphology of *Lingulodinium polyedrum* (Dinophyceae) in culture. PhD Thesis, University of Westminster, London.

Harland, R., 1977. Recent and Late Quaternary (Flandrian and Devensian) dinoflagellate cysts from marine continental shelf sediments around the British Isles. Palaeontographica Abteilung B Paläophytologie 164, 87–126.

Head, M.J., Seidenkrantz, M.-S., Janczyk-Kopikowa, Z., Marks, L., Gibbard, P.L., 2005. Last Interglacial (Eemian) hydrographic conditions in the southeastern Baltic Sea, NE Europe, based on dinoflagellate cysts. Quaternary International 130, 3–30.

Heim, C., 2005. Die Geochemische Zusammensetzung der Sedimente im Aralsee und Sedimentationsprozesse während der letzten 100 Jahre. Diploma thesis, Alfred-Wegener-Institut Bremerhaven.

Hensen, V., 1887. Über die Bestimmung des Planktons oder des im Meere treibenden Materials an Pflanzen und Thieren. Berichte der Kommission zur wissenschaftlichen Untersuchung der deutschen Meere in Kiel 5, 107.

Issar, A.S., Govrin, Y., Geyh, A.M., Wakshal, E., Wolf, M., 1990. Climate changes during the upper Holocene in Israel. Israel Journal of Earth Sciences 40, 219–223.

Kloosterboer-van Hoeve, M.L., Steenbrink, J., Brinkhuis, H., 2001. A short-term cooling event, 4.205 million years ago, in the Ptolemais basin, northern Greece. Palaeogeography, Palaeoclimatology, Palaeoecology 173, 61–73.

Kokinos, J.P., Anderson, D.M., 1995. Morphological development of resting cysts in cultures of the marine dinoflagellate *Lingulodinium polyedrum* (=*L. machaerophorum*). Palynology 19, 143–166.

Kotlyakov, V.M., Serebryanny, R., Solomina, O.N., 1991. Climate change and glacier fluctuation during the last 1000 years in the southern mountains of the USSR. Mountain Research and Development 11 (1), 1–12.

Kouli, K., Brinkhuis, H., Dale, B., 2001. *Spiniferites cruciformis*: a fresh water dinoflagellate cyst? Review of Palaeobotany and Palynology 133, 273–286.

Kunz-Pirrung, M., 1998. Rekonstruktion der Oberflächenwassermassen der östlichen Laptevsee im Holozän anhand von aquatischen Palynomorphen. Berichte zur Polarforschung 281, 1–117.

Kunz-Pirrung, M., 1999. Distribution of aquatic palynomorphs in surface sediments from the Laptev Sea, Eastern Arctic Ocean. In: Kassens, H., Bauch, H.A., Dmitrenko, I., et al., (Eds.), Land–Ocean Systems in the Siberian Arctic: Dynamics and History. Springer-Verlag, Berlin, pp. 561–575.

Landmann, G., Reimer, A., Lemcke, G., Kempe, S., 1996. Dating late glacial abrupt climate changes in the 14,570-yr long continous varve record of Lake Van, Turkey. Palaeogeography, Palaeoclimatology, Palaeoecology 122, 107–118.

Leegaard, C., 1920. Microplankton from the Finnish waters during the month of May 1912. Acta Societatis Scientiarum Fennicae 48, 1–44.

Lemcke, G., Sturm, M., 1996. ^{18}O and trace element measurements as proxy for the reconstruction of climate changes at Lake Van (Turkey). In: Dalfes, H.N., Kukla, G., Weiss, H. (Eds.), Third Millenium BC; Climate Change and Old World Collapse, NATO ASI Series I vol. 49. Springer Verlag, pp. 653–678.

Létolle, R., Mainguet, M., 1993. Aral. Springer Verlag, Paris.

Lewis, J., Hallett, R., 1997. *Lingulodinium polyedrum* (*Gonyaulax polyedra*) a blooming dinoflagellate. Oceanography and Marine Biology: An Annual Review 35, 97–161.

Lioubimtseva, E., 2002. Arid environments. In: Shahgedanova, M. (Ed.), Physical Geography of Northern Eurasia. Oxford University Press, Oxford. 571 pp.

Maev, E.G., Karpychev, Yu, A., 1999. Radiocarbon dating of bottom sediments in the Aral Sea: age deposits and sea level fluctuations. Water Resources 26/2, 187–194.

Marret, F., Zonneveld, K.A.F., 2003. Atlas of modern organic-walled dinoflagellate cyst distribution. Review of Palaeobotany and Palynology 125, 1–200.

Marret, F., Leroy, S., Chalié, F., Gasse, F., 2004. New organic-walled dinoflagellate cysts from recent sediments of Central Asian seas. Review of Palaebotany and Palynology 129, 1–20.

Matthiessen, J., Kunz-Pirrung, M., Mudie, P.J., 2000. Freshwater chlorophycean algae in recent marine sediments of the Beaufort, Laptev and Kara Seas (Arctic Ocean) as indicators of river runoff. International Journal of Earth Sciences 89, 470–485.

Meunier, A., 1910. Microplankton des Mers de Barents et de Kara. Charles Bulens, Imprimerie Scientifique, Bruxelles.

Mirabdullayev, I.M., Joldasova, I.M., Mustafaeva, Z.A., Kazakhbaev, S.K., Lyubimova, S.A., Tashmukhamedov, B.A., 2004. Succession of the ecosystems of the Aral Sea during its transition from oligosaline to polyhaline conditions. Journal of Marine Systems 47, 101–107.

Mudie, P.J., 1992. Circum-arctic Quaternary and Neogene marine palynofloras: paleoecology and statistical analysis. In: Head, M.J., Wrenn, J.H. (Eds.), Neogene and Quaternary Dinoflagellate Cysts and Acritarchs. American Association of Stratigraphic Palynologists, Foundation, Dallas, TX, pp. 347–390.

Mudie, P.J., Aksu, A.E., Duman, M., 1998. Late Quaternary dinocysts from the Black, the Marmara and Aegean seas: variations in assemblages, morphology and paleosalinity. In: Smelror, M. (Ed.), Abstracts from the Sixth International Conference on Modern and Fossil Dinoflagellates Dino 6, Trondheim, June 1998, Norges teknisk-naturvitenskapelige universitet Vitenskapsmuseet, Rapport botanisk serie vol. 1998-1.

Mudie, P.J., Aksu, A.E., Yasar, D., 2001. Late Quaternary dinoflagellates cyst distribution. Review of Palaebotany and Palynology 125, 1–200.

Mudie, P.J., Rochon, A., Aksu, A.E., Gillespie, H., 2002. Dinoflagellate cysts, freshwater algae and fungal spores as salinity indicators in Late Quaternary cores from Marmara and Black seas. Marine Geology 190, 203–231.

Mukhamedshin, K.D., 1977. Tien Shan juniper forests and their economic significance (Archevniki Tian'-Shanya I ikh lesokhoziaistvennoye znacheniye). Ilim, Frunze.

Nehring, S., 1994. Spatial distribution of dinoflagellate resting cysts in recent sediments of Kiel Bight, Germany (Baltic Sea). Ophelia 39, 137–158.

Nourgaliev, D.K., Heller, F., Borisov, A.S., Hajdas, I., Bonani, G., Iassonov, P.G., Oberhänsli, H., 2003. Very high resolution paleosecular variation record for the last 1200 years from the Aral Sea. Geophysical Research Letters 30 (17), 4-1–4-4.

Nurtaev, B., 2004. Aral Sea Basin evolution: geodynamic aspect. In: Nihoul, J.C.J., Zavialov, P.O., Micklin, Ph.P. (Eds.), Dying and Dead Seas: Climatic Anthropic Causes. Proceedings of the NATO Advanced Research Workshop, Liège, Belgium, 7–10 May, 2003, Nato Science Series: IV. Earth and Environmental Sciences vol. 36. Springer-Verlag, Berlin, pp. 91–97.

Parra Barientos, O.O., 1979. Revision der Gattung *Pediastrum* Meyen (Chlorophyta). Bibliotheca Phycologia 48 (1-186), 1–55.

Popescu, S.-M., 2001. Végétation, climat et cyclostratigraphie en Paratéthys centrale au Miocène supérieur et au Pliocène inférieur d'après la palynologie. Thèse de doctorat, Université Claude Bernard—Lyon 1.

Popescu, S.-M., in press. Upper Miocene and Lower Pliocene environments in the southwestern Black Sea region from high-resolution palynology of DSDP site 380A (Leg 42B). Palaeogeography, Palaeoclimatology, Palaeoecology.

Reimer, P.J., Baillie, M.G.L., Bard, E., Bayliss, A., Beck, J.W., Bertrand, C.J.H., Blackwell, P.G., Buck, C.E., Burr, G.S., Cutler, K.B., Damon, P.E., Lawrence Edwards, R., Fairbanks, R.G., Friedrich, M., Guilderson, T.P., Hogg, A.G., Hughen, K.A., Kromer, B., McCormac, G., Manning, S., Bronk Ramsey, C., Reimer, R.W., Remmele, S., Southon, J.R., Stuiver, M., Talamo, S., Taylor, F.W., van der Plicht, J., Weiyhenmeyer, C.E., 2004. IntCal04 terrestrial radiocarbon age calibration, 0–26 cal. yr BP. Radiocarbon 46 (3), 1029–1058.

Rochon, A., de Vernal, A., Turon, J.-L., Matthiessen, J., Head, M.J., 1999. Distribution of Recent Dinoflagellate Cysts in Surface Sediments from the North Atlantic Ocean and Adjacent Seas in Relation to Sea-Surface Parameters. American Association of Stratigraphic Palynologists, Contributions Series No. 35, pp. 1–150.

Savoskul, O.S., Solomina, O.N., 1996. Late Holocene glacier variations in the frontal and inner ranges of the Tien Shan, central Asia. The Holocene 6 (1), 25–35.

Schilman, B., Ayalon, A., Bar-Matthews, M., Kagan, E.J., Almogi-Labin, A., 2002. Sea–land palaeoclimate correlation in the eastern Mediterranean region during the Late Holocene. Israel Journal of Earth Sciences 51, 181–190.

Shirinov, T., Alimov, K., Baratov, S., Rakhimov, K., Saparov, N., Boroffka, N., Vjunnemann, B, Rajnkhardt, Khr., Sorrel, P. and Krivonogov, S., 2004. Polevye raboty po proektu INTAS Aral No. 00-130: "Klimaticheskie izmenenija v epochu golocena i razvitie poselenij cheloveka v bassejne Aral'skogo Morja" "Holocene climatic variability and evolution of human settlement in the Aral Sea basin (CLIMAN)". Arkheologicheskie issledovanija v Uzbekistane 2003 goda, 4, 197–205.

Tarasov, P.E., Webb III, T., Andreev, A.A., Afanas'eva, N.B., Berezina, N.A., Bezusko, L.G., Blyakharchuk, T.A., Bolikhovskaya, N.S., Cheddadi, R., Chernavskaya, M.M., Chernova, G.M., Dorofeyuk, N.I., Dirksen, V.G., Elina, G.A., Filimonova, L.V., Glebov, F.Z., Guiot, J., Gunova, V.S., Harrison, S.P., Jolly, D., Khomutova, V.I., Kvavadze, E.V., Osipova, I.M., Panova, N.K., Prentice, I.C., Saarse, L., Sevastyanov, D.V., Volkova, V.S., Zernitskaya, V.P., 1998. Present-day and mid-Holocene biomes reconstructed from pollen and plant macrofossil data from the

former Soviet Union and Mongolia. Journal of Biogeography 25, 1029–1053.

Tchepaliga, A., 2004. Late Glacial great flood in the Black Sea and Caspian Sea. Geological Society of America Annual Meeting, Seattle, 2–5 November 2003, Abstract, session No 189.

Velichko, A.A., 1989. The relationship of the climatic changes in the high and low latitudes of the Earth during the Late Pleistocene and Holocene. In: Velichko, A.A., et al., (Eds.), Paleoclimates and Glaciation in the Pleistocene. Nauka Press, Moscow, pp. 5–19.

Wall, D., Dale, B., 1966. "Living fossils" in Western Atlantic plankton. Nature 211 (5053), 1025–1026.

Wall, D., Dale, B., 1974. Dinoflagellates in late Quaternary deep-water sediments of the Black Sea. In: Degens, R.T., Ross, D.A. (Eds.), The Black Sea—Geology, Chemistry and Biology, Memoir vol. 20. American Association of Petroleum Geologists, pp. 364–380.

Wall, D., Dale, B., Harada, K., 1973. Description of new fossil dinoflagellates from the Late Quaternary of the Black Sea. Micropaleontology 19, 18–31.

Wünnemann, B., Riedel, F., Keyser, D., Reinhardt, C., Pint, A., Sorrel, P., Oberhänsli, H., submitted for publication. The limnological development of the Aral Sea since the early Middle Ages inferred from sediments and aquatic organism. Quaternary Research.

Zavialov, P.O., 2005. Physical Oceanography of the Dying Aral Sea. Springer Verlag, Chichester, UK. 146 pp.

Zavialov, P.O., Kostianoy, A.G., Emelianov, S.V., Ni, A.A., Ishniyazov, D., Khan, V.M., Kudyshkin, T.V., 2003. Hydrographic survey in the dying Aral Sea. Geophysical Research Letters 30 (13), 2.1–2.4.

Zech, W., Glaser, B., Ni, A., Petrov, M., Lemzin, I., 2000. Soils as indicators of the Pleistocene and Holocene landcsape evolution in the Alay Range (Kyrghystan). Quaternary International 65/66, 161–169.

Zonneveld, K.A.F., Versteegh, G.J.M., de Lange, G.J., 2001. Palaeoproductivity and post-depositional aerobic matter decay reflected by dinoflagellate cyst assemblages of the Eastern Mediterranean S1 sapropel. Marine Geology 172, 181–195.